Metrology for energy harvesting
European Metrology Research Programme

EURAMET
European Association of National Metrology Institutes

FINAL PUBLISHABLE JRP REPORT

JRP-Contract number	ENG02
JRP short name	Harvesting
JRP full title	Metrology for Energy Harvesting
Version numbers of latest contracted Annex Ia and Annex Ib against which the assessment will be made	Annex Ia: V2.1 (11 July 2013) Annex Ib: V2.0
Period covered (dates)	From 01 09 2010 to 31 08 2013
JRP-Coordinator	
Name, title, organisation	Jürgen Melcher, Dr., PTB
Tel:	+49 531 592 2100
Email:	juergen.melcher@ptb.de
JRP website address	http://projects.npl.co.uk/energy_harvesting/
Other JRP-Partners	
Short name, country	CMI, Czech Republik INRIM, Italy LNE, France MIKES, Finland NPL, United Kingdom SIQ, Slovenia

Report Status: PU Public

EMRP
European Metrology Research Programme
Programme of EURAMET
The EMRP is jointly funded by the EMRP participating countries within EURAMET and the European Union

TABLE OF CONTENTS

1 Executive Summary

Energy harvesting is the generation of small scale energy from ambient sources such as movement, vibration or waste heat, either in the environment or resulting from human activity. It provides high value energy at the point of use that can be used to power electronic devices indefinitely, free from wires and/or batteries. Applications include industrial monitoring, medical implants, “smart” energy distribution, traffic and asset control, and wearable electronics. By recycling energy such as waste heat from vehicle exhausts, energy harvesting can also improve efficiency, reducing fuel consumption in cars by 5-10 %.

This project developed European metrology capability to support the commercial development of the energy harvesting market, including support for emerging new technologies at the micro- and nano-scales.

The Problem

Our modern technological society relies increasingly on the massively widespread use of low power devices for communications and information technology. Providing power to wireless devices presents a significant challenge that could be addressed with the harvesting of ambient sources of energy. This could eliminate the need for wired power connections or expensive and polluting batteries in many applications. On a larger scale, improved efficiency through waste heat harvesting could make significant reductions in energy usage, and CO2 emissions, particularly in the automotive sector.

European industry has made strong growth in energy harvesting for industrial monitoring and building controls. However, there is unrealised potential for energy harvesting to achieve wider mass-market adoption (estimated to be worth €5 billion by 2022). A major reason for this is uncertainty over performance expectations within the supply chain and a lack of measurement infrastructure and consistent performance metrics both for existing as well as emerging new technologies.

The Solution

To realise the full potential of the energy harvesting market, and a strong position for European companies, a number of metrological challenges need to be addressed. Energy harvesters typically generate weak and distorted signals which are difficult to measure. Traceable measurement of harvested power and generic definitions and metrics of terms such as efficiency, effectiveness and power output are required to prevent confusion in the market. Agreed methods for specifying performance parameters (efficiency, power, power density) or their measurement for vibration harvesters are required. Very large measurement uncertainties and a lack of reference materials, for thermoelectric harvesters, particularly at elevated temperatures need to be reduced. Robust traceable measurement for emerging new materials and energy conversion technologies, including nanotechnologies is lacking needs to be implemented.

The Impact

The results of our research are being taken up by industry in a number of ways. Morgan Advanced Materials, a global materials engineering company, are using our research help them develop standardised energy harvesting metrics, to provide their customers with a clear understanding of the output of a device in their environment. We have worked with a FTSE 100 global engineering company to apply the measurement facilities developed in the project to energy harvesters under development by the company. Input from the project was requested for the development of energy harvesting performance metrics for ISA100.18 (International Society of Automation) power sources standards committee. Broader standards participation is being discussed within IEC/TC 113 and IEC TC47. This uptake of project output with companies, and input into the development of standards in this area will help communication within the supply chain based on reliable performance metrics.

This project has also had a direct input to new developments in related areas. The Piezoselex “Piezoelectric Pair Materials for the Selective Exclusion of Workplace Noise” is a Research for SME’s, European Seventh Framework project for the development of an improved device for the prevention of noise induced hearing loss builds on capability developed under this project. A French industry consortium composed of Thales Systems Avionic, Dassault Systems and four SMEs is developing vibration energy harvesters for autonomous sensors for aircraft monitoring, will use capability developed in this project. The development of a high temperature thermoelectric reference material will provide the basis for traceable measurement services to industries in the near future.

2 Project context, rationale and objectives

Our modern technological society relies increasingly on the massively widespread use of low power devices for communications and information technology. The proliferation of portable electronic devices has seen massive growth in wireless technologies, set to grow exponentially as a wider range of devices become connected (the Internet of Things).

Providing power to these wireless devices presents a significant challenge. Power is currently supplied by batteries or inefficient voltage converters. A recent EU policy statement states 'The EU market for batteries amounts to approx. 800,000 tonnes of automotive batteries, 190,000 tonnes of industrial batteries and 160,000 tonnes of consumer batteries every year. These batteries contain metals, which might pollute the environment at the end of their life-cycle. Mercury, lead and cadmium are seen as the most dangerous substances [1]. The potential for reduction in small primary battery utilisation addresses EC Directive 2006/66/EC (Batteries directive) [2]. The primary objective of this Directive is to minimise the negative impact of batteries and accumulators and waste batteries and accumulators on the environment. This research project directly addresses the policy objectives of reducing the numbers of primary batteries through the deployment of energy harvesting strategies. This reduction of primary batteries will minimise the disposal of batteries and accumulators as mixed municipal waste as laid down in Article 7 of the directive.

Energy harvesting could eliminate the need for wired power connections or expensive and polluting batteries in many applications. An energy harvester, operating for a lifetime of 20 years would generate the energy contained in roughly 70 standard primary button cells. On a larger scale, improved efficiency through waste heat harvesting could make significant reductions in energy usage, and CO2 emissions, particularly in the automotive sector.

The energy sources of interest to this research project were the largely untapped sources of ambient energy resulting from human activity and environmental energy flows in the form of waste heat, movement and vibration. The energy sources of interest range from the medium energy range (W to kW) – for example heat transfer from automotive exhaust gasses used to recharge the battery - down to meeting the low power requirements (µW to mW) of portable electronics and mobile communications. For thermal converters, the technology of most interest commercially and in research is thermoelectric conversion. For harvesting energy from movement or vibration electromagnetic, piezoelectric, magnetostrictive and electrostatic energy harvesters were of major interest.

European industry, supported by investment in research and development, has made strong growth in energy harvesting for industrial monitoring and building controls. However, there is unrealised potential for energy harvesting to achieve wider mass-market adoption (estimated to be worth €5 billion by 2022). A major reason for this is uncertainty over performance expectations within the supply chain and a lack of common metrics. Technology providers are unsure what information to provide to their customers, and potential users are unsure which technology to use, or whether the technology will work with their application. This problem is exacerbated by performance inflation where a high level of competition, unsupported by reliable measurement standards leads to inflated performance claims based on incompletely specified measurement conditions.

There are generic problems that need to be addressed in the traceable measurement of power and related electrical quantities. Energy harvesters typically produce low level, distorted and intermittent electrical signals for which there was a lack of techniques for their traceable measurement. There are also measurement issues relating to specific energy sources such as very large uncertainties in the measurement of the thermoelectric figure of merit, even for bulk materials, and a lack of reference materials, particularly for high temperatures required by the automotive industry. For vibration energy harvesting, concepts such as efficiency or power density were poorly defined, and numbers obtained vary greatly depending on how the measurement is conducted. These problems are compounded at the micro and nano-scales. Most of the major automotive companies are engaged in development of thermoelectric generators for harvesting energy from waste heat from the vehicle exhaust. New materials are being developed for this market where control of the structure at the nanoscale has the potential to significantly increase performance and reduce cost. However, prior to this project techniques for the traceable quantification of thermal and electrical properties at the nanoscale did not exist. Similarly with piezoelectric converters there are emerging new nanostructured materials. Even in conventional piezoelectric materials, their performance is determined by their structure and properties at the nanoscale. These effects become significant even in microscale devices where domain processes in ferroelectric materials can be influenced by shape and form. MEMS (Micro Electro Mechanical System) energy harvesters are a rapidly emerging technology with significant progress towards commercialisation in recent years in the US and in Europe, and there is a need for new techniques for measuring energy coupling, electrical and mechanical properties at these length scales.

The overall scientific and technological objective of the project was to provide, within Europe, the metrological framework, technical capability, and scientific knowledge to enable the development of effective and commercially successful energy harvesting technologies. This ranges from the use of known technology in novel ways, to the development of new technologies and materials to meet the growing market demand for energy harvesting. This project addressed three main challenges in energy harvesting metrology:

1. Power from energy harvesting is usually on a small scale and is intermittent in nature. The signals from energy harvesters are not clean sine waves that we can measure very accurately but they are noisy signals of varying profiles. Thus, existing measurement techniques are not adequate for measuring the weak and distorted signals generated by most energy harvesters.
2. There are challenges relating to particular energy harvesting technologies. For vibrational or motion energy harvesting, there is a lack of agreed definitions and metrics of terms such as efficiency, effectiveness or power output. This can lead to widely varying reported metrics that have little bearing on what could be achieved in practice, and confusion in the market. The measurement of the performance of thermoelectric converters for waste heat recovery is also subject to very large measurement uncertainties, and a lack of reference materials, particularly at elevated temperatures.
3. There is a drive to develop ever smaller energy harvesting devices that can be integrated with the electronics they are powering, and to exploit emerging new nano-technologies for energy harvesting. This requires the development of suitable techniques for performance characterisation at the nano-scale. By providing robust traceable measurement for emerging new materials and energy conversion technologies, this will help accelerate the development of new products, new applications, and new commercial opportunities for energy harvesting

To address these challenges, this project had the following scientific and technological objectives:

Objective 1 To develop the metrology framework to provide traceable and reliable measurement of thermal, mechanical and electrical properties that relate to the transduction of thermal or vibrational energy into useful electrical quantities.

- For vibration and motion harvesting this requires the capability to reliably and traceably map performance under varying conditions encountered in practical situations (performance mapping).
- For thermoelectric harvesting, new techniques are required to provide more accurate measurements and reference materials for industry, particularly at elevated temperature.

Objective 2 To develop measurement definitions and techniques for the characterisation of efficiency and power output in energy harvesters, allowing industry to compare technologies and techniques.

Objective 3 To develop traceable techniques for the measurement of small AC and DC electrical quantities with complex waveforms typical of energy harvesting applications.

Objective 4 To establish measurement techniques for the characterisation of thermal and mechanical energy transduction at the micro- and nano- scales.

3 Research results

This section summarises the results of the research conducted in this project. These results address the project objectives as follows:

Objective 1 To develop the metrology framework to provide traceable and reliable measurement of thermal, mechanical and electrical properties that relate to the transduction of thermal or vibrational energy into useful electrical quantities.

- For vibrational or motion energy harvesting, methods for specifying performance parameters (efficiency, power, power density) and their measurement are described in Section 3.4
- New techniques have been developed to provide more accurate thermoelectric measurements and reference materials for industry at elevated temperature. These are described in section 3.2

Objective 2 To develop measurement definitions and techniques for the characterisation of efficiency and power output in energy harvesters, allowing industry to compare technologies and techniques.

- Definitions and metrics of terms such as efficiency, effectiveness and power output relating to energy harvesting are described in Section 3.1.

Objective 3 To develop traceable techniques for the measurement of small AC and DC electrical quantities with complex waveforms typical of energy harvesting applications.

- Energy harvesters typically generate small distorted and intermittent electrical output. Research into the traceable measurement of small non-sinusoidal electrical quantities is presented in Section 3.5.

Objective 4 To establish measurement techniques for the characterisation of thermal and mechanical energy transduction at the micro- and nano- scales.

- Research into measurement of thermoelectric properties at the nanoscale is described in Section 3.3
- Developments in measurement techniques for MEMS scale mechanical energy harvesters and methods for measuring energy coupling at the nanoscale are described in Section 3.4.

3.1 Conversion efficiency of microgenerators, converting thermal or mechanical energy into electrical energy

3.1.1 *Section Introduction*

The efficiency with which energy can be converted from mechanical or thermal sources to useable electrical energy is a major factor in the design of an energy converter. Low efficiency means that more energy must be extracted from the source to provide the energy required for any particular application. High loading of the energy source can adversely affect the energy source. For example, high thermal conductivity in a thermoelectric converter using waste heat from a vehicle exhaust will cool the exhaust gasses resulting in back-pressure that affects engine operation. Presenting an excessive load when harvesting from human motion, e.g. walking, will tire the person. Low efficiency also means that the energy conversion device may need to be bigger, and use more materials to deliver a given amount of electrical energy. Efficiency is therefore an important parameter in most energy harvesting applications.

This section presents research relating to the measurement of efficiency in energy harvesters (Objective 2). Modelling of the conversion efficiency of mechanical to electrical energy harvesters is presented in Section 3.1.2. The application of this modelling to piezoelectric energy harvesters and comparison with experimental measurements is presented in Section 3.1.3. Section 3.1.4 presents a measurement system for the determination of the thermoelectric figure of merit, *ZT* (closely related to the efficiency) using the van der Pauw method for measurement of both thermal and electrical quantities. Efficiency measurements for magnetostrictive (MST) energy harvesters are presented in Section 3.1.5.

3.1.2 *Model for the determination of conversion efficiency of microgenerators*

Mathematical modelling of energy harvesters is complex because of the differing designs, discrepancy of technical data of materials and different types of generators. Each type of generator also has its own benefits for a certain type of application and it is very difficult to make a precise mathematical model which will describe all types of vibrational generators simultaneously, particularly while different conversion mechanisms (from vibration to electricity) are used. Here we describe and explain only one type of vibrational harvester, specifically the piezoelectric generator. The reason is that it gives at its output a noticeably higher electrical power than some other types of harvesters, and is therefore an interesting device for commercial use. This section reviews existing modelling approaches for piezoelectric energy harvesters, and the development of a numerical model based on these approaches. This model was then applied to a particular device configuration, to provide numerical data for comparison with experiment in section 3.1.3.

There are publications where various approaches of energy harvesting devices were studied. First Williams and Yates [4] and then Roundy [5] gave mathematical models which reasonably represent vibration energy harvesting devices (electromagnetic, piezoelectric, MST and electrostatic) however these models have high measurement uncertainty. The publications introduced and investigated a parameter of efficiency or measure of performance η and concluded some definitions. The concept of efficiency should be defined because this gives us an amount of input mechanical harmonic excitation energy that can be converted to usable electrical energy.

Simplified mathematical model

An equivalent model of a piezoelectric harvesting device is shown in fig. 1. General constitutive equations according to IEEE, 1978 for piezoelectric material in cantilever mode can be described with:

$$T_1 = c_{11}^E S_1 - e_{31} E_3 \tag{1}$$

where T_1 is the axial stress, S_1 axial strain component, c_{11}^E elastic stiffness at constant electrical field E_3, e_{31} is the piezoelectric constant.

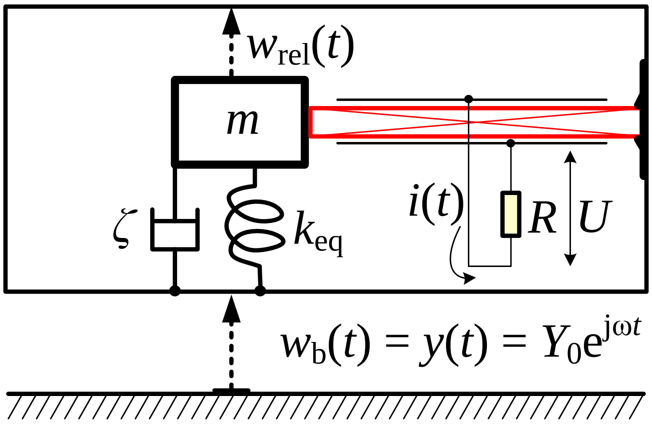

Fig.1. Equivalent model of piezoelectric generator

The operating principle of a piezoelectric conversion device is shown in fig. 1. This is a basic second-order spring-mass-damper-piezo system. If the seismic mass *m* is much smaller than the mass of the harmonic excitation shaker, then this system with vibrating force *y*(t) around its resonance frequency ω_n creates a displacement w_{rel}(t) of mass *m* from its stationary position relative to the source of vibrations with amplitude |*W*|. The restoring spring has an effective stiffness k_{eq} and the damping coefficient ζ.

Usually this spring-mass system has a resonance frequency at a certain natural frequency ω_r of the system, so the quality factor *Q* can be introduced as:

$$Q = \frac{w_{rel}(t)}{w_b(t)} = \frac{m \cdot \omega_n}{\zeta} \tag{2}$$

where *Q* is related to damping constant ζ shown in Fig. 1.

The parameter *Q* describes the degree to which the effect of excitation energy is amplified by a piezoelectric generator as the frequency of excitation approaches the harvester resonant frequency ω_n. This amplification is a property of the body storing the energy and releasing it in phase with the driving energy. The higher the *Q* factor, the more pronounced this amplification effect will be.

The amplitude of displacement *W* of the spring can be described as $W=Q\cdot Y_0$, where Y_0 is the amplitude of input vibrations. If the amplitude of input acceleration can be given by $A=\omega^2\cdot Y$ then the spring deflection can be written as:

$$|W| = \frac{Q \cdot A}{\omega^2} \tag{3}$$

Using general expression for output power [8], a simplified result for maximum output power near the resonant frequency $\omega_r=\omega$ of piezoelectric generator, can be expressed as:

$$P_{\max} = \frac{k^2 m (Q \cdot A)^2}{4 \cdot \omega} \tag{4}$$

The output power of a piezoelectric generator is dependent on the *Q* factor, which is predominantly influenced by the damping constant ζ, total mass *m* and coupling coefficient *k*. Power can be maximised by lowering the damping and increasing the mass *m* and amplitude Y_0 of excitation.

These considerations can be applied to other types of vibration harvesting devices [12], for instance to MST and electrostatic applications. This single degree of freedom (SDOF) model can provide a good starting point for a comparison of wide range of generators however clarification problems with SDOF modelling of piezoelectric energy harvesters was presented in a paper from Erturk and Inman [6]. This is particularly characteristic for piezoelectric systems, where in operating conditions, they are prone to show backward coupling effect throughout piezoelectric crystal activity. The effect of piezoelectric coupling cannot be exactly predicted with viscous damping and damping coefficient ζ. Therefore equation 4 is not appropriate because this equation does not take all relevant design properties into account. It is usually only good for modelling in the early stage of the design process or when comparing different design methods.

The coupled parameter model which describes the behaviour of model shown in fig. 1 can be described with two equations described in [5] as follow:

$$\sigma_{in}(t) = L \cdot \ddot{S}(t) + R_b \cdot \dot{S}(t) + \frac{S(t)}{C_k} + n \cdot u(t),$$
$$i(t) = C_b \dot{u}(t) + \frac{u(t)}{R_l} \qquad (5)$$

Each of the mechanical properties of the mechanical subsystem in fig. 1 is replaced by an equivalent electric component. The electrical current is through variable analogous to the strain rate $\acute{S}$ and bending input stress $\sigma_{in}=k_1 \cdot m \cdot w_{rel}'' = k_1 \cdot f(t)$ is across variable analogous to the input voltage $\sigma_{in}(t)$. The equivalent inductance $L=k_1 \cdot k_2 \cdot m$ relates to the second derivative of strain and represents the mass or inertia of generator where k_1 and k_2 are the geometrical constants [5]. The resistance R_b represent the mechanical damping coefficient b and C_k the compliance (relates strain and stress) or the inverse of the Young modulus Y_p.

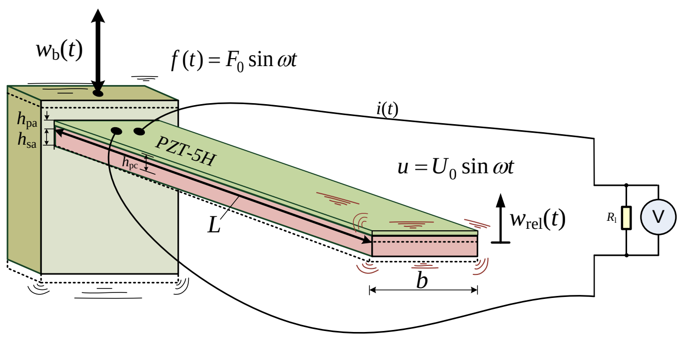

Fig. 2. Piezoelectric cantilever generator excited by translational harmonic input

A model represented by equation (5) represents coupled mechanical-electrical approach to model piezoelectric energy generation. A lumped parameter model represented by equation (5) is shown in fig. 3 and is a widely used approach for modeling piezoelectric harvesters. The electrical side of this model is represented with the equivalent capacitance C_b of piezoelectric bender and electrical load R_l connected on the output of piezoelectric harvester. The characteristic of the piezoelectric harvester is that deformation of piezoelectric material or mechanical energy generates electrical energy. A harmonic input stress in the mechanical domain is related to change of output voltage $u(t)$ across the output of the piezoelectric device on the electrical side.

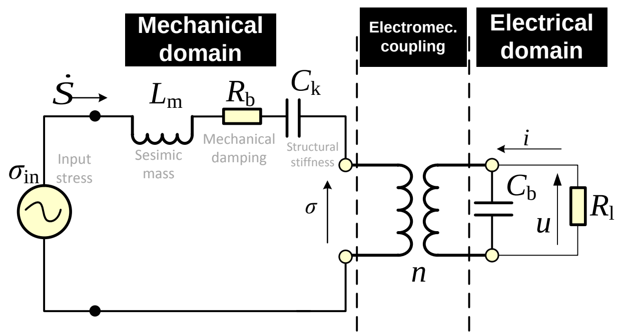

Fig. 3. Lumped equivalent model of piezoelectric harvester

This method of modelling is often used, and here sandwiched layers of piezo-electrodes make an internal bender capacitance C_b. The values of lumped parameters for representation of mechanical area should be estimated [7], to obtain additionally better representation of mechanical domain, a transformer with ratio n is used which represents the voltage feedback to the mechanical domain. Interesting behaviour occurs when load resistance R_l deliberately changes from lower toward higher values. In combination with capacitance C_b in piezoelectric generator, the characteristic point of resonance frequency ω_r shift to higher frequencies.

The problem of changing resonant frequency ω_r is closely related to impedance matching of electrical load to internal source impedance of piezoelectric generator. Internal impedance of piezoelectric harvesters has real and imaginary parts. Also the electrical load R_l (practically, this is an impedance Z) will have real and imaginary parts. In order to scavenge maximum energy from a piezoelectric harvester, a conjugate complex matching of source impedance should be initially achieved. When this condition is not fulfilled (the most common case), we will always have an imaginary component of power which will swing between source and load. Only the real component of load impedance Z is converted to some other form of energy (one part is dissipated in the air and another harvested on R_l). In the same manner, if all of that energy cannot be harvested, then the backward pulsating imaginary part of energy will modify the equivalent model properties of the piezoelectric harvester (particularly varying the reactance of capacitance C_b).

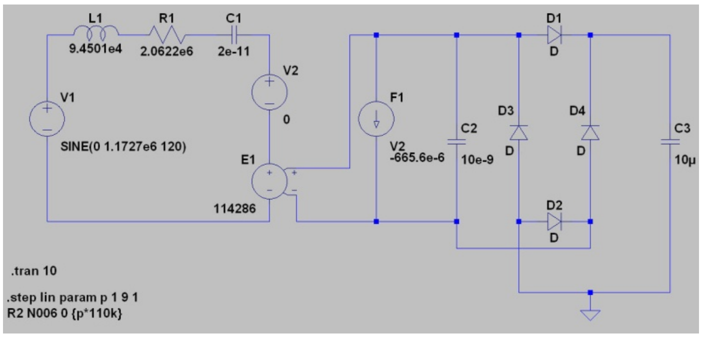

Fig. 4. Spice model of cantilever bimorph piezoelectric generator DuraAct P-876.A11

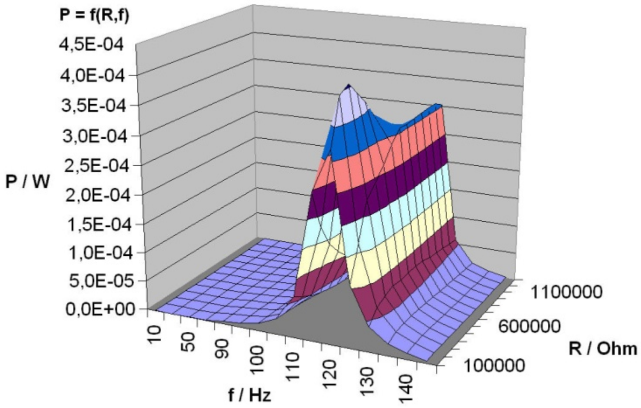

Fig. 5. Electrical power as a function of load resistance (100kΩ – 1,3MΩ) and frequency (10 Hz -150Hz)

As a consequence, in the two extreme cases, when in the first case the impedance of load is infinity and in second is zero, a piezoelectric generator will show maximum voltage at open-circuit resonance frequency f_{oc} and maximum output current at short-circuit frequency f_{sc}. The curve of electrical power tends to be similar as predicted with equation (4). Equation (4) states that harvested power P_{max} always increases when the coupling coefficient k increases. In fig. 5, we can conclude that the surface has two peaks; in frequency and also in resistance domain, two maxima and one minimum. For simplicity we will briefly describe why this happens, [8] and say that for generators with a small damping coefficient ζ and a strong coupling coefficient k the system tends to have two peaks in power near the resonant frequency ω_r. The output power first increases, then decreases, because the displacement at the tip mass also first increases and then decreases. This means that with increasing frequency, displacement decreases and then overall output power is reduced. That also means that electrical output power is nonlinear and directly proportional to ζ and k.

As theoretically and experimentally proved in [7] this lumped parameter model is much more useful in describing the dynamic behavior of piezoelectric harvesters than the previous expression (4) [4]. However, this model also has some weak points. In the model shown in fig. 2 it is assumed that the mass of the piezoelectric cantilever can be neglected compared to the proof mass m. If the proof mass m is not greater than the mass of the cantilever beam (while it is even worst when it does not exist), this model will also generate noticeably large errors in the estimation of the output electrical power. Therefore, after two attempts, it was decided to use the distributed parameter model. The coupled distributed model proposed by Erturk and Inman [6] for unimorph piezoelectric cantilever beams was used for explanation of problematic piezoelectric systems.

In fig. 2 unimorph cantilever piezoelectric generator with all relevant physical quantities are shown. This configuration (31 modes) achieves the best power output because a piezoelectric film bonded on substrate and coupled in transverse direction provides the best mechanical amplification of the applied excitation. This type of generator was used and commonly described in the literature, because it can give the output electrical power. The layers of piezoelectric materials were fixed (glued) on a metallic cantilever to obtain a desired common resonant frequency (for this type of the generator it is in the range from 10 Hz to 300 Hz). For the experimental set-up we have used this type of piezoelectric generator for further examinations. A piezoelectric tape manufactured by the company PI (DuraAct P-876.A11, piezoceramic PIC 252) glued on an aluminium cantilever represents a one such type of generator that was investigated.

3.1.3 *Application to piezoelectric harvesters*

The accuracy of amplitude and shape of curve as calculated from the mathematical model, was compared with the results obtained from the measurements on a piezoelectric generator. The mechanical and electrical properties of the unimorph piezoelectric generator used in the experiment are shown in table 1. The measurement set-up for the determination of output power and efficiency is shown in fig. 6.

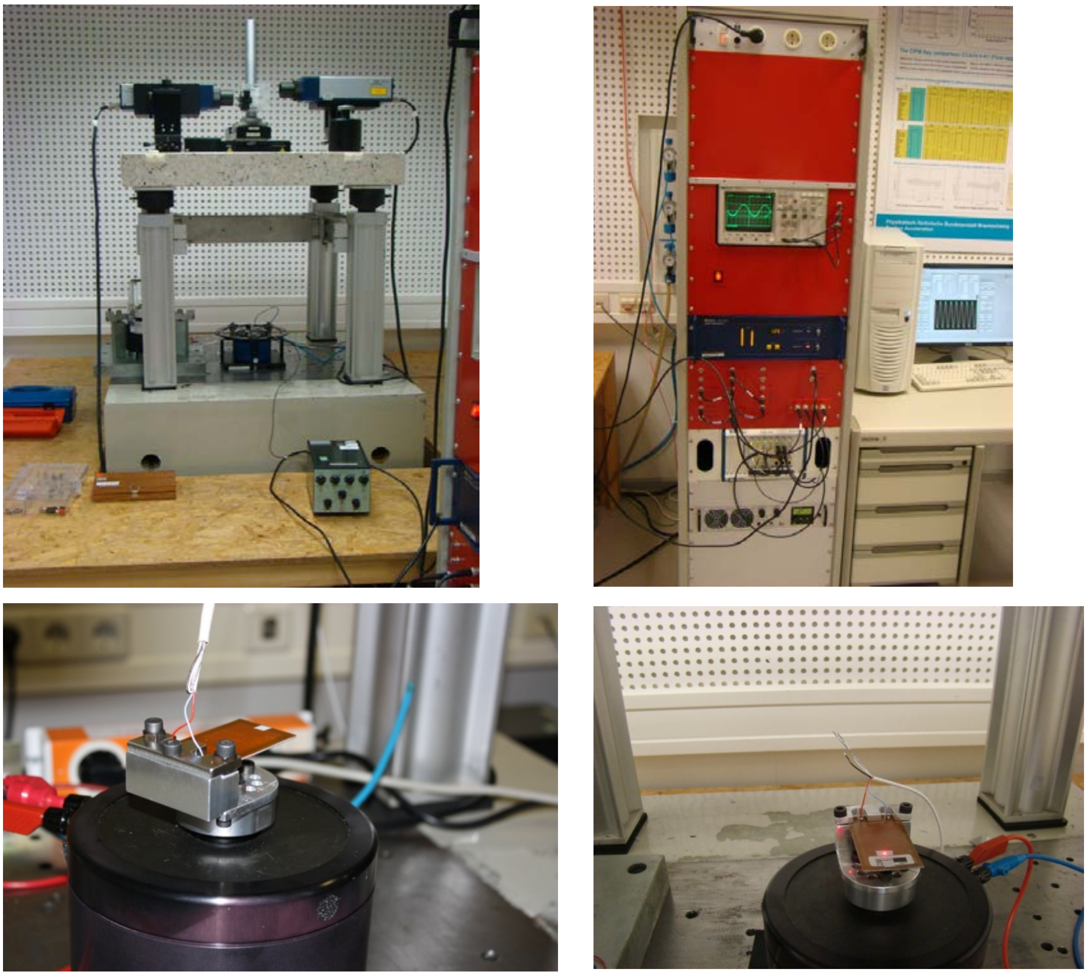

Fig. 6. Experimental set-up for testing of output power and efficiency of piezoelectric generator

The first version of piezoelectric generator was constructed to work around a resonant frequency ω_r=ω_1=835,66 rad/s. With fixed values of load resistance R_l and input acceleration a, results are shown in fig. 7. We see that mathematical and experimental results show a good agreement with a small discrepancy in amplitude, resulting in an absolute error of approximately -6 %.

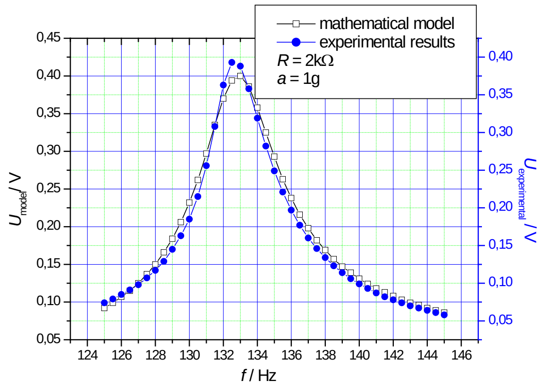

Fig. 7. Voltage output of piezoelectric generator where blue dots represent experimental results and black a result given by mathematical model

With this first sample of piezoelectric generator we did not take any more results due to a lack of a proper measurement set-up and mechanical generator design. Testing of generator output electrical power at higher accelerations unintentionally led to plastic deformations and the mechanical properties of the generator changed.

In a second attempt we produced a new version of a piezoelectric generator (cantilever was made from thicker aluminium). In fig. 8 are shown experimental results for second generator, with resonant frequency ω_r≈1828,4 rad/s. The value of acceleration was measured with the help of laser interferometers. Acceleration and load resistance was constant during measurement process. The stability of a constant value of acceleration was > 0.5 %, therefore the contribution to the error can be found in a somewhat unstable acceleration measurement loop. In fig. 8 it can be seen that the absolute error is somewhat smaller, but it is necessary to emphasise that after more measurement iterations, this error tended to be bigger (this lead as to conclusion that aluminium shim changed its mechanical properties again).

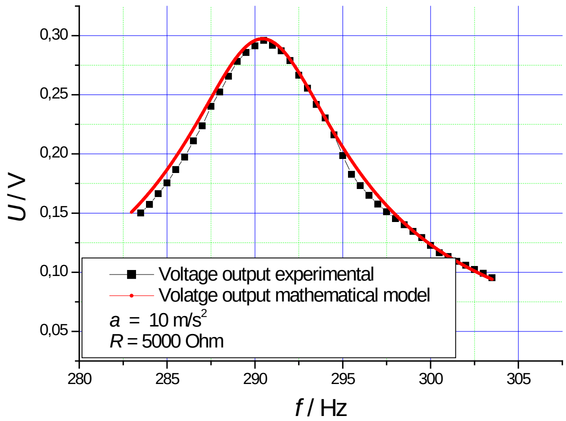

Fig. 8. The voltage dependence of the frequency obtained from mathematical model and experimental results

Power output dependency is depicted at fig. 9. The real measured power P_{out} generated at load resistance R_l can be calculated using following equation:

$$P_{out} = \frac{V^2}{R_l}, \tag{6}$$

where V represent maximum voltage or peak amplitude of AC voltage in stationary state at the output of piezoelectric generator.

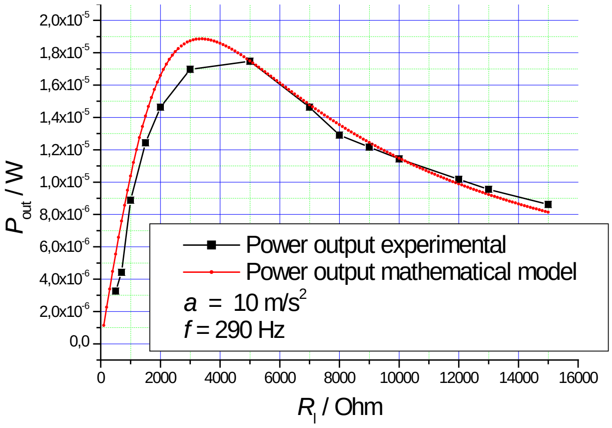

Fig. 9. Compared output electrical power from mathematical model and experimental results at load resistance R_l

At the resonance state, the produced electrical power was in the range of tens of microwatts. This power is not sufficiently large for commercial applications, but for validation purpose of the mathematical model, it is sufficient.

The discrepancy between mathematical and experimental results for power output was in the range of 10 %. We used a resistance decade box (calibrated with uncertainty less than ±1 %) as a load resistor, to investigate impedance matching effect on piezoelectric generator. Intentionally, we have not used AC/DC converters, capacitors or diodes to avoid efficiency estimation of this additional device.

In the measurement set-up shown in fig. 6 we did not use a force sensor for measurement of dynamic input force and therefore the efficiency of piezoelectric generator for the first time was mathematically calculated using next equation:

$$\eta = \frac{V^2/R_l}{F \cdot v} = \frac{P_{out}}{M \cdot a \cdot \omega \cdot Y_0}, \tag{7}$$

where M is the mass of piezoelectric generator, ω resonant angular frequency and Y_0 the amplitude of displacement given by laser interferometers.

In the last measurement experiment we investigated efficiency η of second piezoelectric generator using equation (7). The first results of experiment are shown in fig. 10.

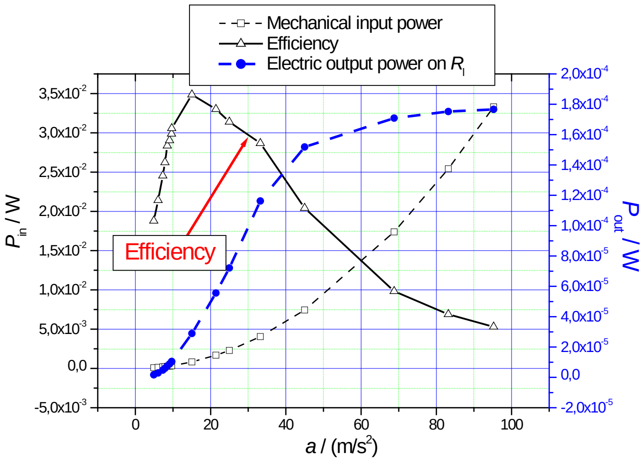

Fig. 10. Efficiency of piezoelectric generator given by output power divided by input mechanical power

It can be seen that for mechanical input power determined as product of force *F* and velocity *v* applied to the generator (black dashed line), the output electrical power P_{out} increases almost linearly until 40 m/s^2. Furthermore it goes in saturation and more input mechanical power does not imply also more electrical output power. Interestingly, calculated efficiency (solid black triangle symbol line) rises linearly until the maximum at 13 m/s^2 and then gradually decreases. It shows us that the *maximum of efficiency does not imply also a maximum of output power* of generator.

This experiment gave rise to the idea that efficiency η is not the best quantity for describing the quality or level of effectiveness of generator under consideration. From the perspective of a consumer, maximum power output or power output density (W/cm^3) makes more sense because it gives more power in smaller dimensions. However, we must note that both piezoelectric generators have shown quite stable material characteristics only in the weak acceleration regime. At higher amplitudes of vibration, the forces and acceleration are greater therefore electrical power output is also greater. However, excessive stressing of the system will lead to degradation of material properties, or device failure. This has important metrological and testing implications because the power output stated for a device may have been measured under conditions that are not compatible with reliable operation over a long lifetime. This is particularly of concern for piezoelectric devices, because they are often supplied as unpackaged piezoelectric components that have not been engineered for a particular application. Whilst there are some very reliable and highly engineered electromagnetic products on the market (e.g. Perpetuum), the issues of reliability and lifetime testing and prediction are in their infancy for many piezoelectric and other new technology energy harvesters. This is an important topic for future research, but beyond the scope of the present project.

3.1.4 ***Measurement system for the determination of ZT with the van der Pauw method***

Using the Van der Pauw (VdP) method it is possible to measure the conductivity of square shaped samples of materials used for construction of thermoelectric generators (TEG). The conductivity σ is determined by measurements of the so called VdP resistances and by measurements of the thickness of the sample. The terminus VdP resistance is shown in fig. 11 and defined as follows: if the edges of the square sample were counter clockwise numbered as 1, 2, 3, and 4, the VdP resistance R_{12} is the ratio of the voltage drop across the edges 3-4 and the current through the edges 1-2. By a cyclic rotation of the current and voltage connections to the edges of the sample four different measurements can be made. By presuming a perfect sample (homogenous conductivity; square plate with the large surfaces being parallel) the four resistance measurements give equal results. The samples used have the dimension of approximately 5 $\times$ 5 $\times$ 5 mm^3. Contact to the corners of the quadratic plates should be made by pressing metallic plates at an angle of 45 degrees against the four 2 mm long edge lines as it is shown in fig. 12.

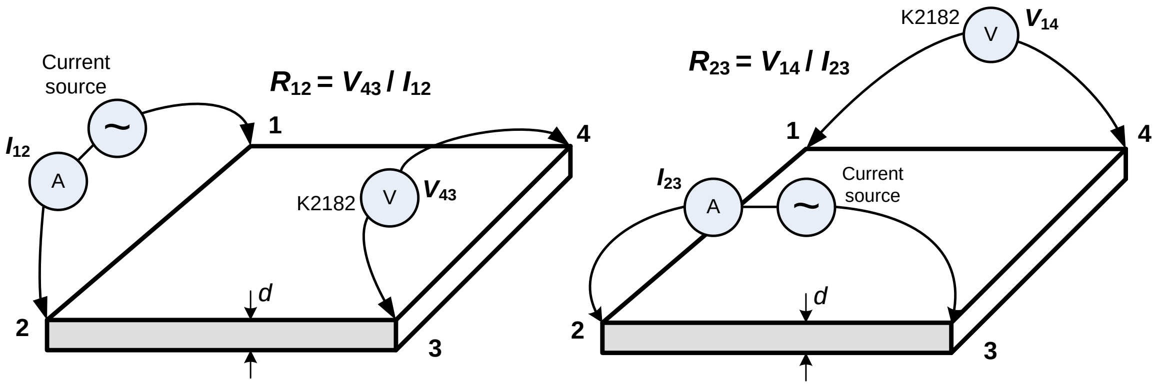

Fig. 11. Van der Pauw measurement of electrical conductivity

The electrical conductivity σ can be determined from VdP measurements using the equation

$$\frac{1}{\sigma} = \frac{\pi \cdot d}{\ln(2)} \cdot \frac{R_A + R_B}{2} \cdot f(r) \quad (8)$$

In equation (8), R_A and R_B are the mean values $R_A = (R_{12} + R_{34})/2$ and $R_B = (R_{23} + R_{41})/2$, d is the thickness of the plate and $f(r)$ is a correction factor which takes into account that the plate possibly is not perfectly quadratic so that the ratio $r = R_A / R_B \neq 1$. The advantage of the VdP method is that only one dimensional measurement – the measurement of the thickness d is necessary. It is evident from equation (8) that the uncertainty of the determined conductivity is essentially influenced by the uncertainties of the thickness d and of the resistances R_A and R_B.

Complete characterisation of thermoelectric materials can be done with the previously described methodology [16]. Using the novel thermal vdP method it is possible to simultaneously measure Seebeck coefficient, electrical and thermal conductivity. This can be done using three resistance/thermometer heaters H2 – H4 as shown in fig. 12. These heaters serve as thermal sources and it is also possible to directly measure temperature at these points of the sample. Furthermore, with the same methodology shown in fig. 11, the values of thermal resistances K_{12}, K_{23}, K_{34} and K_{41} can be simultaneously measured. Thermal current across thermoelectric material will also produce potential difference between probes E1 – E4 so the Seebeck voltage can be measured. This measurement method has yet another advantage, as parallel sets of measurements via proper switching and use of bipolar current source can be done, which gives the ratio of AC (achieved with low frequency bipolar switching) and DC resistance of the sample being tested.

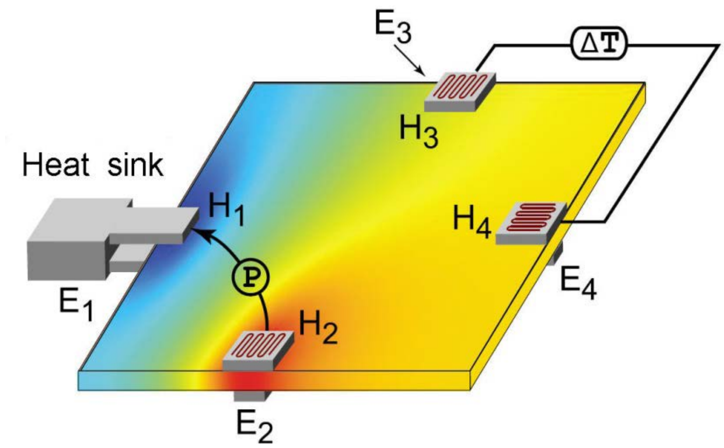

Fig. 12. Van der Pauw measurement of electrical, thermal conductivity and Seebeck voltage

This ratio is important for calculating ZT using the Harman method. It should be noted that all measurements were performed using true four-terminal measurement and therefore contact resistances do not affect the final result. Currently, the measurement uncertainty of measuring ZT using a combined vdP approach is approx. 5-10 %.

Thermal conductivity, electrical conductivity and Seebeck coefficient were measured using the measurement head shown in fig 13.

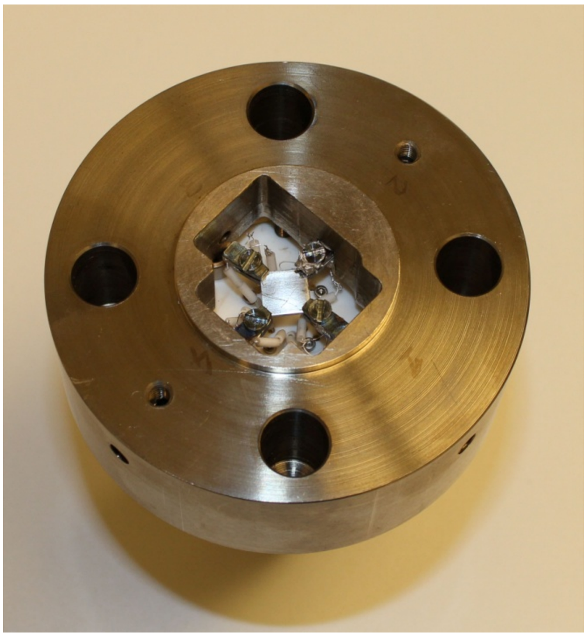

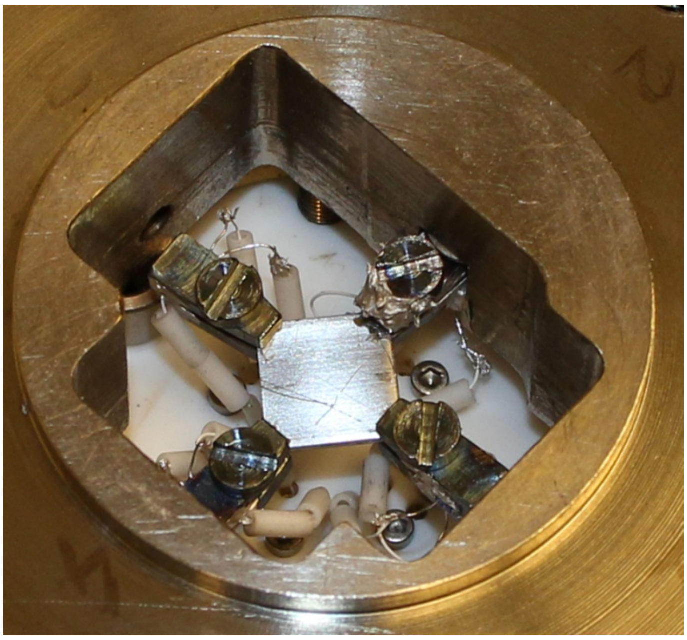

Fig. 13. Measurement VdP head

This is an improved version of measurement adapter and provides additional heat guarding (radiation from sample material to the environment is greatly reduced and electrical contacts were made using four mechanical clamps). The advantage of this measurement adapter is that it offers better stability and measurements of all three quantities at higher temperatures (up to 700K).

3.1.5 *Efficiency measurement in magnetostrictive energy harvesters*

The work on a magnetostrictive (MST) harvester was mainly performed by INRIM. Such work focused on the following issues:

- Realisation and validation of a simulation tool suitable for the performance and efficiency analysis of MST devices.
- Realisation of a MST harvester
- Realisation of measurement set-up for MST harvesters
- Analysis of the parameter of influence of the performance and efficiency of a MST device.

The research focused on stress driven MST harvesters, such as how the force exerted by the vibration, acts directly on the active material. The vibration, in this type of device, can be induced by a mechanical component in which the generator is inserted. Such a component can be an automotive suspension, a part of a machine tool, or, the harvester can be part of the supporting elements of a vibrating mass. The frequency for these applications is in the order of hundreds of hertz therefore we focused on an intermediate frequency of 300 Hz.

A simulation tool for MST generators, simulating energy conversion, was tuned and validatedat INRIM. Through the implementation of a step by step procedure, the instant of time magnetisation and strain were computed by implementing a coupled finite element – magnetoelastic model. The software received as input the characteristics of the active material (measured and identified), the preload provided to the active material (measured), the mechanical excitation (the harmonic force impressed to the device, measured), the parameters of the coil pick up coil and the electrical resistance of the load and, finally, the parameters of the bias magnet (permanent magnets). As an output the software provides the time behavior of the electrical current at the load and, if the characterisation of the material is complete, the time-behavior of the displacement. The software allows the comparison between measurements and simulations, improves the design phase devoted to MST devices and allows the analysis of parameter which influences the performance and the efficiency. Among the latter, some were harder to be analysed by measurements: e.g. the level of magnetisation of magnets. A study on an amorphous ribbons based harvester, developed during the project, was published taking advantage from the developed tool (M. Zucca, O. Bottauscio, Modeling Amorphous Ribbons in Energy Harvesting Applications, IEEE Trans. Magn., 47, 2011, p. 4421-4424).

The prototype MST generator is a device which converts mechanical into electrical energy. The realisation of this device is linked to the need of having a real device on which to perform investigations. Currently, there are several electromagnetic and piezoelectric devices on the market, however MST devices are relatively new. Moreover the realisation of a prototype of MST generator is needed in order to perform some basic validations of the simulation software. The device is able to provide an output power up to 81 mW at 300 Hz, with a sinusoidal stress variation having peak of 2.75 MPa (the specific power in this case is slightly higher than 5 mW/cm^3).

Prototype device description: A rod of MST material constituted of bulk $Tb_{0.3}Dy_{0.7}Fe_{1.92}$ is inserted in a pickup coil, this latter connected to an electric impedance (pure resistive). Two NdFeB permanent magnets provide the magnetic bias. The material is preloaded with a constant stress, whilst a time varying mechanical load is exerted longitudinally along the rod axis. The pick-up coil has a larger diameter with respect to the rod, and is suspended in order to avoid friction between the coil and the active material (Fig. 14). (M. Zucca, O. Bottauscio, Hysteretic Modeling of electrical Micro-Power Generators Based on Villari Effect. IEEE Trans. Magn., vol. 48, 2012, p. 3092-3095)

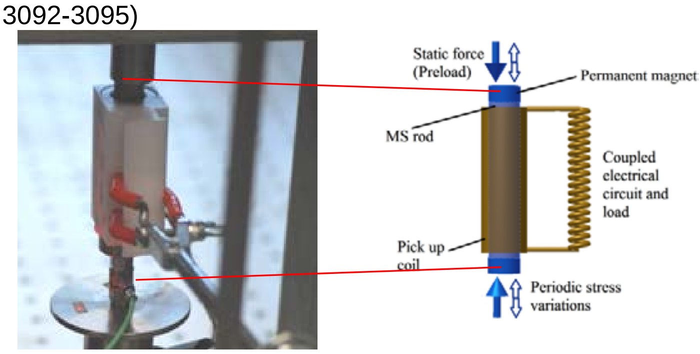

Fig.14. Microgenerator inserted in a test rig. On the right side: principle scheme

A new system was set-up at INRIM in order to measure the performance and the efficiency of a vibrational MST harvester based on bulk materials (Fig. 15). Efforts were made to stabilise the generation of mechanical power (input vibration), which eventually turned out to have negligible variations.

The set-up provided:

1. a static preload to the active material;
2. a dynamic vibrational force to the MST material, with a profile as close as possible to a-sinusoid;
3. an electric load as output of the device.

The set-up allowed the measurement of:

4. the electrical power on the electrical load;
5. the mechanical power in input to the harvester.

Moreover the set-up avoided:

6. undesired resonances in the frequencies of interest (up to some hundreds of hertz);
7. mechanical instabilities or drift.

The set-up included an optical breadboard with a frame made of non-magnetic steel. The harvester was hosted inside the frame. The coupling between the frame parts is obtained by eight M8 screw, tightened so as to make the friction between the parts negligible. The frame has a hole to allow a vibrometer beam to reach the target. The frame also included a nut and lock nut for the preload creation and a fully controlled piezoelectric actuator, with a feedback control able to produce a vibration having a nearly sinusoidal force profile.

The measurement system was made by components inside the set-up and by external hardware. Components inside were: the load cell and target disk for the laser beam. Components outside were: the load cell amplifier; laser vibrometer head and decoder, digital precision multimeter, PXI system which includes the ADC converter for acquisition, the analog outputs for the excitation control, standard resistors for manual measurements and PXI programmable resistors for automatic measurements and a CPU including a M card controlling the PXI and including the Labview™ software which manages the measurements.

The system is able to provide electrical measurement with a relative standard uncertainty of approx. 10^{-3}. However, due to the complexity of the dynamic mechanical measurements with preload, the expanded uncertainty in the efficiency measurement is equal to 5.0 % (95 % interval of confidence).

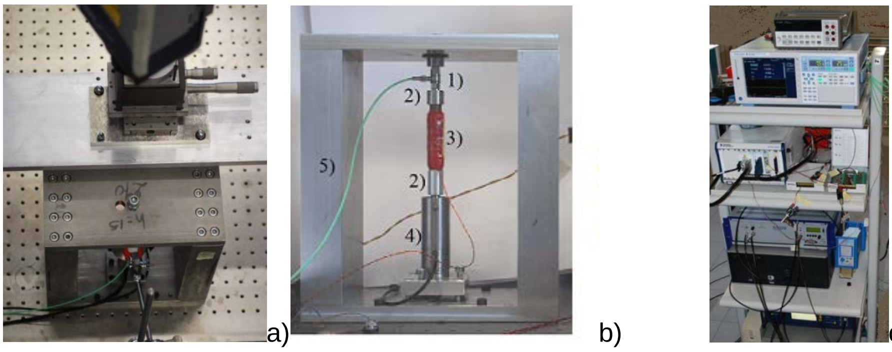

a) b) c)

Fig. 15. Experimental set-up: a) Top view of the system, b) Sistem components
1) load Cell, 2) supports including permanent magnets, 3) coil around the Terfenol D rod,
4) piezoelectric actuator, 5) gantry.
c) Measurement and control system.

The set-up enabled the analysis of the parameter of influence of the performance and efficiency of the MST device with the results shown for various parameters in figures 16-19:

1. We measured the relationship between the output electrical power and the stress amplitude excitation which followed a cubic scaling law (Fig. 16);
2. The electrical characteristics (power vs current) were analysed varying the load at constant mechanical excitation and varying frequency (Fig. 17). We also measured the effect of preload on the performance (Fig. 18)
3. Some efficiency behaviours were investigated (Fig. 19)
4. Performance and efficiency were shown to be to be directly related to the magnetisation bias.

As a conclusion stress amplitude, preload, frequency, electrical load and magnetisation bias have been found to be the key parameters of the efficiency and performance of this kind of harvester. The efficiency of the investigated device is approx. 20 % to 30 %, depending on the active material sample, coupled circuit and quality of bias magnets. Some preliminary investigations were made of the effects of friction between the active material and the coil. These showed that friction significantly modifies the harvester efficiency and strongly affects the measurement repeatability, but detailed investigation was beyond the scope of the present project.

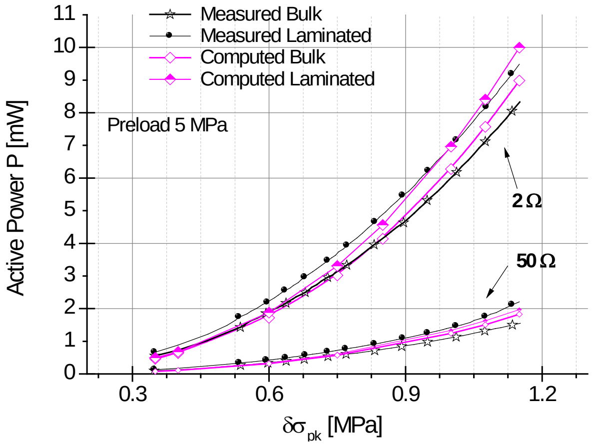

Fig. 16. Active electric power provided by the generator as a function of the variable stress amplitude. The variation follows approximately a cubic law.

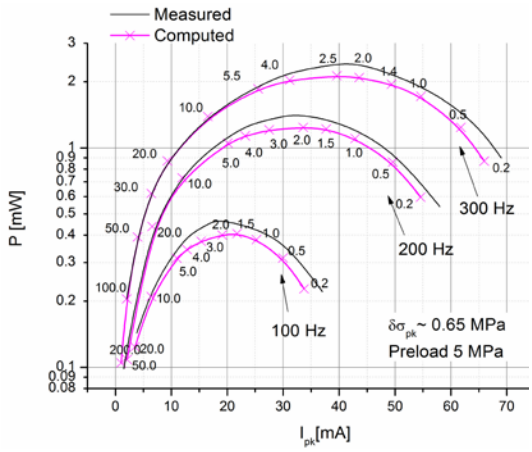

Fig. 17. Load curve of the generator for different frequencies. The values of the load resistance in Ω are reported as labels on the curves

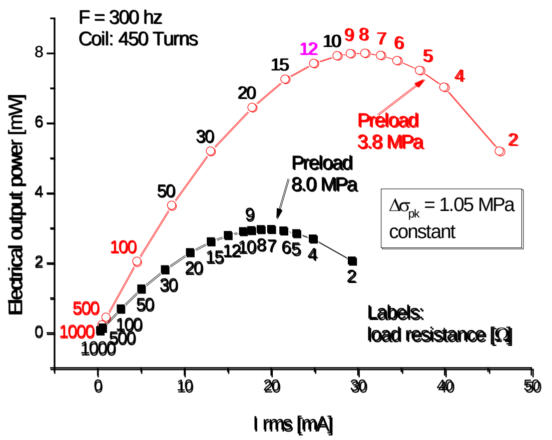

Fig. 18. Load curve of the generator for two different preload values. The values of the load resistance in Ω are reported as labels on the curves.

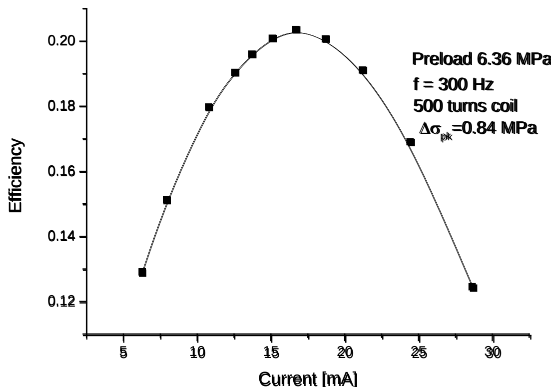

Fig. 19. Effect of the electrical load on the efficiency

3.1.6 ***Section Summary***

This section presents research relating to the measurement of efficiency in energy harvesters (Objective 2). Results are presented on the definition and measurement of performance and efficiency in piezoelectric, thermal and magnetostrictive energy harvesters, supported by modelling and measurement data. The key outputs from the research reported in this section are:

- Models were developed for the measurement of power and conversion efficiency in micro-generators and applied to piezoelectric energy harvesters, showing good agreement between theory and experiment. Where the energy harvester presents a small load to the vibrating system, the efficiency is not of paramount concern and measurement of power density under well-defined conditions is required. However, in some applications the power available from the vibration source is limited and the harvester draws a significant proportion of this power. In these cases, efficiency becomes an important factor in the operation of an energy harvester.

- The efficiency and power output of a thermoelectric energy harvester are defined by the thermal conductivity, electrical conductivity and Seebeck coefficient. A new capability for measurement of these coefficients, based on the van der Pauw method, is demonstrated, providing measurements of the thermoelectric figure of merit up to 700 K.
- New results are presented on the power output and efficiency of magnetostrictive (MST) harvesters. The research focused on stress driven MST harvesters where the stress is directly applied, with potential applications such as automotive suspension, or machine tools. A new facility for traceable determination of power and efficiency of direct force MST harvesters is described. A new software tool was developed to accurately simulate the non-linear behaviour of MST harvesters and to predict performance as a function of various input parameters.
- The parameters that influence performance and the efficiency of direct force MST harvesters were determined and their analysis is presented above.

3.2 Figure of merit of macroscopic thermoelectric reference materials

3.2.1 Section Introduction

The aims of this work were the development of precise and traceable measurement methods and systems for the determination of the Seebeck coefficient S, the electrical conductivity σ, and thermal conductivity κ of macroscopic thermoelectric bulk materials. This work addresses Objective 1: new techniques for thermoelectric measurements, to provide more accurate measurements and reference materials for industry, particularly at elevated temperature.

These transport properties are relevant for the efficiency of the energy transformation of thermoelectric materials which is expressed by the figure of merit ZT, defined as $ZT= S^2\sigma T/\kappa$. A high ZT-value of a material is an indicator of a high efficiency of the conversion of thermal energy into electrical energy and - vice versa. Furthermore reference materials for Seebeck coefficients should be developed and characterised to get an undisputed instrument of known thermoelectric properties, which is essential to validate testing methods and to allow the reliable benchmarking of different thermoelectric materials. Furthermore, a reference material is an adequate instrument to validate measuring systems and methods used to measure complex quantities like the Seebeck coefficient.

After agreeing on the concept for the measuring facilities and applied techniques in December 2010 the measurement set-ups were developed in PTB and MIKES. In December 2011 a system to measure the Seebeck coefficient and the electrical conductivity of thermoelectric bulk materials and thin films developed and constructed at Fraunhofer IPM [19] was installed and tested at PTB this system further on is named SR5. In the first version the SR5 was equipped with type-K differential thermocouples, but these were replaced by more homogeneous Au/Pt differential thermocouples to reduce uncertainty influences caused by inhomogeneities of the used differential thermocouples. Furthermore, a calibrated Pt-100 thermometer was integrated into the SR5 measuring system to get traceability to SI units of the temperature measurement.

3.2.2 Results

The schematic measurement set-up of the measuring system is shown in Fig. 20. The temperature depending Seebeck coefficients and electrical conductivities of the samples were measured in a protection gas atmosphere of nitrogen (N_2) or forming gas at a pressure of (30-60) mbar. Promising results, particularly concerning the reproducibility of the Seebeck coefficient measurements were achieved. The good reproducibility and the thermal stability of metallic alloys at high temperatures supports the use of metallic alloys as reference materials for Seebeck coefficients rather than the use of semiconductors, particularly at temperatures above 650 K.

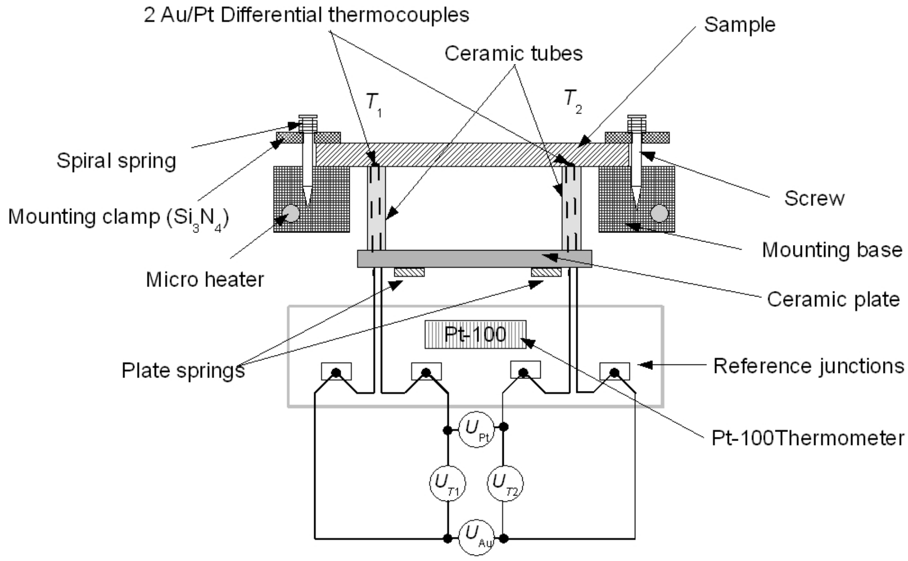

Fig. 20. Schematic measuring arrangement at PTB to measure the Seebeck coefficient

For the measurement the sample was fixed on two mounting bases each equipped with a micro-heater at a set a temperature gradient (1 K – 8 K) above the sample. The two small differential Au/Pt thermocouples were mechanically pressed against the sample from below by using thin spring blades made of tungsten. The thermocouples were used to measure the temperatures T_1 and T_2 and, therefore, the mean sample temperature T_S, as well as the temperature difference ΔT across the sample. Furthermore, the two congeneric thermoelements of the differential Au/Pt thermocouples were used to measure the voltages U_{Au} and U_{Pt} (see Fig. 20), which were used to calculate the unknown Seebeck coefficient S_X of the sample according to equation 1 by using the slopes a_{Au} and a_{Pt} of the linear regression of the value pairs $U_{Au}/\Delta T$ and $U_{Pt}/\Delta T$, and by taking into account the absolute Seebeck coefficients of the thermoelements (S_{Au} and S_{Pt}):

$$S_x = \frac{1}{2}\left[\frac{a_{Au}+a_{Pt}}{a_{Pt}-a_{Au}} \cdot S_{Au/Pt} + S_{Au} + S_{Pt}\right] \tag{1}$$

The temperature of the sample, T_S, was calculated on basis of measurements of the reference temperature T_{Ref} close to the sample temperature by using the calibrated Pt-100 resistance thermometer as well as the two Au/Pt differential thermocouples according to equation 2:

$$T_S = T_{Ref} + \Delta T_{DiffTE}, \tag{2}$$

with ΔT_{DiffTE} << T_{Ref}. In keeping T_{Ref} and the sample temperature close to each other, the mean sample temperature could be measured traceably and with a high accuracy.

The whole arrangement was inserted into the measurement chamber which could be evacuated and filled with inert gases. For measurements at different temperatures, the sample and the holder were heated up by using a cylindrical and sheathed heater that surrounded the whole sample holder. An additional cartridge heater was used to set the reference temperature T_{Ref}.

The relative measurement uncertainties in measuring the Seebeck coefficient were in the order of a few percent. The uncertainty contributions of the slopes a_{Au} and a_{Pt} (equation 1) were the largest ones caused by the calculation of the regression lines and the uncertainty of the voltage measurement. However some more investigations were necessary to reduce these influences.

The relative measurement uncertainty of the electrical conductivity by using the four terminal method was found to be approx. 5 - 6 % (k = 2) for the metallic alloys. The main contributions were the uncertainties of the dimensional measurements of the sample in particular the uncertainty according to the length (distance between the differential thermocouples).

A 3 ω measurement system was developed at MIKES for determining the thermal conductivity of bulk samples from room temperature up to 725 K. The thermal conductivity measurements were performed in a horizontal three-zone tube furnace whose sample space can be evacuated to vacuum or alternatively a protective argon gas environment can be applied to prevent undesired oxidation and contamination of the sample material. After validating the system with known dielectric, semiconductor and metal samples, it was used for measuring several thermoelectric samples. The thermal conductivity values of the measured test samples covered a wide range from 0.37 $W \cdot m^{-1} \cdot K^{-1}$ to 150 $W \cdot m^{-1} \cdot K^{-1}$. We also implemented an extension of the 3 ω method which includes a prefabricated sensor deposited on a stand-alone Kapton plate. Such a transferable sensor allows for faster and simpler thermal conductivity measurements (up to 425 K) without the need to deposit the metal heater and potentially a dielectric layer on every new sample. The relative measurement uncertainty in thermal conductivity measurements using the 3 ω method was between 4 % and 8 % (k = 2).

As reference materials for the Seebeck coefficients PTB recommended ISOTAN® and bismuth-doped lead telluride in the temperature range from 300 K to 860 K and 300 K to 650 K respectively.

ISOTAN® was chosen because of its thermal stability over the whole temperature range and easy handling (mechanically stability etc.). Combined with its good availability and high homogeneity according to thermoelectric effects it compensates its relatively low Seebeck coefficient and makes therefore a good thermoelectric reference material. The high homogeneity allowed a certification process according to the ISO Guide 35. The recommended size of the ISOTAN® samples is 0.3 mm, 3 mm, and 25 mm (height, width, and length, respectively). The values are given due to needed stability and proper handling. The homogeneity of the Seebeck coefficient of the used batch of ISOTAN® was evaluated by performing a random test. The mean Seebeck coefficient measured at approx. 303 K was calculated on basis of 11 samples. The value was found to be -37.22 µV/K with a standard deviation of 0.33 µV/K; which justified a certification of the whole batch according to the ISO Guide 35. The short term measurements of the Seebeck coefficients were performed on 30 randomly chosen samples, 10 samples were stored in a refrigerator at a temperature of approximately -25 °C, 10 under laboratory conditions, and 10 in a climate cabinet at a temperature of 50 °C and 10 % humidity. The samples were measured before and after storing (maximum storing time 90 days). All measurements were performed at a temperature of T = 303 K. Each Seebeck coefficient was measured three times and the resulting mean value was taken as result of the measurement. The measured Seebeck coefficients show deviations by approx. 1 % after storing at -25 °C and at room temperature and by approx. 1.5 % after storing at 50 °C. This may be caused by an exchange of the Au/Pt thermocouples of the measuring system in the mean time, but was considered as one uncertainty contribution as well as the homogeneity of S. The investigation of the long term stability of the ISOTAN® samples is going on (2-3 years required). Fig. 21 shows the temperature dependency of the Seebeck coefficient of ISOTAN® in the temperature range from 300 K to 860 K of 6 different samples measured with data of at least three individual runs, respectively. Also shown is a fit of the Seebeck coefficients by a third order polynomial with a standard error of fit of approx. 0.46 µV/K.

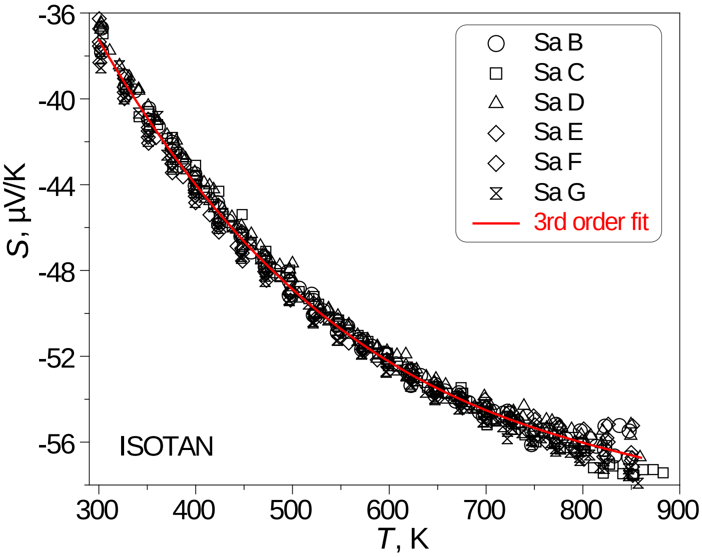

Fig. 21. Measured Seebeck coefficients of six different ISOTAN® samples and a third order polynomial fit

The temperature dependency of the Seebeck coefficient of ISOTAN® in the temperature range from 300 K to 850 K shows a relative uncertainty (*k* = 2) from approximately 8.7 % at 300 K down to approximately 5.5 % at 850 K.

After testing several semi-conducting materials (arsenic-doped germanium, cobalt-doped iron disilicide and bismuth-doped lead telluride) it turned out that bismuth-doped lead telluride (*Bi*-PbTe) offered the best compromise taking into account aging effects and interaction with Au/Pt-thermocouples. Therefore *Bi*-PbTe was chosen as semi-conducting reference material for Seebeck coefficients. Nevertheless we had to reduce the temperature range for its application to ensure optimal measurement results. Due to the limited homogeneity of the Seebeck coefficient and a limited number of samples which not allows a certification according to the requirements of the ISO Guide 35 a certification procedure for each single sample was necessary. Two batches of *Bi*-PbTe (each 19 samples) were purchased with a carrier density of 1.2×10^{19} cm^{-3}. The samples were cut out from two disks of *Bi*-PbTe. The dimensions of the *Bi*-PbTe samples were (15 x 2.5 x 2) mm. The short term stability was tested again by measurements of *S* at approx. 303 K before and after the storage (40-90 days) of the samples at -25 °C, at room temperature and at 50 °C. The measured Seebeck coefficients agree within approx. ±1 %. The long term investigation of the stability of *S* at room temperature is on-going.

Preliminary measurements of *S* by using *Bi*-PbTe samples produced aging effects when heated above 650 K. Therefore, the range for the certification as a reference material for Seebeck coefficients was limited to temperatures between 300 K and 650 K. Furthermore, it was found that the electrical conductivity and on a limited scale the Seebeck coefficient of *Bi*-PbTe depends on a thermal pre-treatment of the samples. An annealing of the samples of approx. two hours at a temperature of 600 - 650 K before the measurements of the Seebeck coefficient is recommended to reduce oxides formed on the surface if stored in air. The Seebeck coefficients of 14 samples of *Bi*-PbTe of one batch were measured. The typical dependency of the Seebeck coefficients of *Bi*-PbTe on temperature is shown in Fig. 22. Data was fitted by polynomials of the third order for each sample

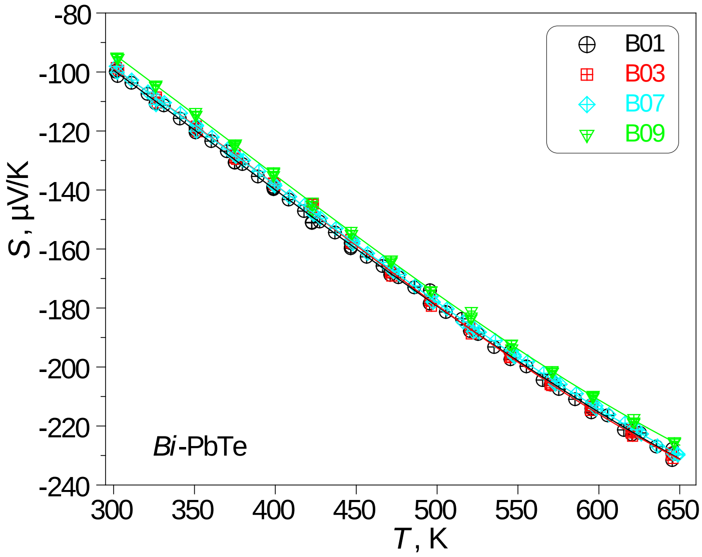

Fig. 22. Measured Seebeck coefficients of four different Bi-PbTe samples and third order polynomial fits of each sample

The temperature dependency of the Seebeck coefficient of *Bi*-PbTe in the temperature range from 300 K to 650 K shows a relative uncertainty (k = 2) of the Seebeck coefficient from approximately 4 % at 300 K down to approximately 2.5 % at 650 K.

3.2.3 *Section Summary*

This section presents the development of new techniques to provide more accurate measurements and reference materials for thermoelectric measurements at elevated temperature (Objective 1).

The measuring system SR5 installed and modified at PTB according to traceability is suitable for performing traceable measurements of the Seebeck coefficient of thermoelectric materials. Two reference materials for Seebeck coefficients were characterised in the temperature range between 300 K and 650 K (*Bi*-PbTe) and between 300 K and 860 K (ISOTAN®). The relative measurement uncertainties (k = 2) obtained of the Seebeck coefficients were in the order of only a few percent. They amount to approx. 4 % for *Bi*-PbTe and to approx. 8 % for ISOTAN® at 300 K and decrease to approx. 2.5 % for *Bi*-PbTe at 650 K and to approx. 6 % for ISOTAN® at 860 K. It is the first time that reliable reference materials for Seebeck coefficients with low uncertainties at temperatures above approx. 400 K were made available to validate measuring systems and methods for Seebeck coefficients and to allow a direct comparison of different thermoelectric materials concerning their Seebeck coefficients.

The measurements of the electrical conductivity on basis of the four-terminal-method by using the SR5 measuring system (simultaneously to the Seebeck coefficient) resulted in relative uncertainties (k = 2) in the same order of magnitude for the Seebeck coefficient in the same temperature ranges for the two different thermoelectric materials. The thermal conductivities were measured at temperatures up to approx. 425 K but with measurement uncertainties of 4-8 %, i.e. slightly better than scheduled.

3.3 Metrology for nanostructured thermoelectrics

3.3.1 *Section Introduction*

Thermoelectric devices are based on carefully chosen semiconductor materials that convert waste heat to electrical energy and vice versa. It is now accepted [13] that the way to increase the energy density exchanged by these devices is by carefully limiting thermal losses in systems and/or by producing better materials.

The efficiency of thermoelectric materials is determined by a so-called figure of merit $ZT = S^2 \sigma T/\kappa$, Where S is the Seebeck coefficient, σ the electrical conductivity, κ the thermal conductivity and T the temperature. For semiconductor materials these properties are inter-related and depend strongly on the precise chemical composition of the materials as well as on the nanostructure of the sample. Careful design and precise chemical fabrication process, coupled to accurate physical characterisation at the nanoscale are therefore required to progress the materials science of this type of materials. NPL and CMI have also used scanning probe microscopy to evaluate the lateral variation of the different transport properties at the nanoscale. Three new techniques were implemented to measure, electrical resistance, thermal conductance and thermopower.

This work relates to Objective 4, the establishment of measurement techniques for the characterisation of thermal energy transduction at the nano- scale.

3.3.2 *Nanoscale Electrical Resistance Measurement*

Current Atomic Force Microscopy (C-AFM) was used to investigate the resistivity of a material. The method consists of measuring the current flowing through a tip after it makes contact through a sample under an electrical bias. By measuring the current, it is possible to calculate the value of resistance of the material, and using spreading resistance equation, the resistivity of the material can also be obtained. However, due to the usual presence of a contamination layer in air or the presence of an oxide on the sample, current – AFM is usually limited to tunnelling current measurement (femto-ampere). This type of measurement is extremely surface sensitive and usually measure trapped charges or surface contamination.

The Scanning Spreading Resistance Mode (SSRM) differs from (C-AFM) in one key aspect: a much higher force is applied to the tip; this results in a pressure at the end of the tip of the order of a few GPa and a contact area much larger than for C-AFM. However, it can be argued that this level of pressure is enough to go through any potential oxide presents on the surface.

SSRM (Fig. 23) was validated for silicon (Si) and is extremely delicate to operate due to the requirement for large deflection of the AFM cantilever – which introduces further instability during the scan. The key for reproducible results in Si is the formation of an ohmic contact between the tip and the sample. Molecular simulations [20] seem to indicate that a structural transformation occurs in silicon during scanning, that transform the Silicon into a semi-metal. Note that quantification is only possible for Si with the help of calibration samples, where the dopant concentration is measured using SIMS.

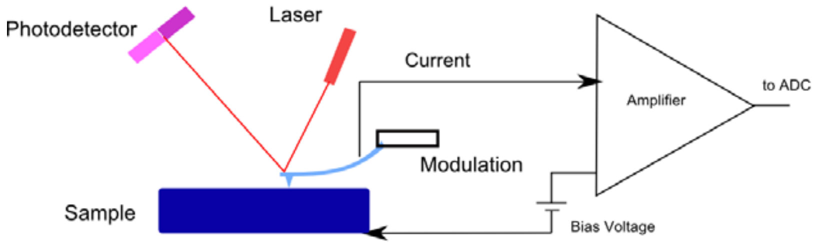

Fig. 23. Schematic of SSRM mode

NPL has developed the following procedure to study the validity of SSRM for thermoelectric materials.

1. The force constant of the cantilever is obtained by measuring its thermal noise
2. We calibrate the displacement sensitivity of the AFM by a force curve on a single crystal sapphire sample. Then check that the sapphire surface is not deformed by scanning the surface
3. A force curve is measured on the material of interest. By comparison with the sapphire force-curve the indentation depth is calculated. We assume that the tip – made of conductive diamond coating- is not deformed under the force applied.
4. The tip size is measured using Scanning Electron Microscopy (SEM) imaging. A Hertzian contact model is used to calculate the contact radius.
5. We first scan the surface of interest with low force and no bias, to ensure that the surface is free of contaminants. A location is then selected
6. Force curve combined with a current distance curve for a given sample bias voltage are acquired

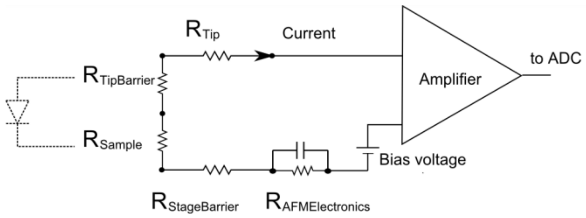

Fig. 24. Approximation of the electrical diagram of SSRM mode

In order to obtain the resistivity from the measured resistance, the electrical contact area must be known. This contact area depends strongly on the force applied by the probe as well as the mechanical properties of the material and local surface conditions. One of largest sources of uncertainty in AFM measurements is the calculation of the spring constant of the probe in order to obtain a force measurement. Using the thermal tune method, this spring constant can have an uncertainty as high as 10 % [21]. We have therefore reached the conclusion that, whilst we can measure current and resistance accurately, the uncertainties in resistivity are too larger.

To assess the lateral resolution of the SSRM technique, we have applied a draft ISO standard method [22] concluding that we can currently achieve a lateral resolution of 30 nm. This is limited by the interaction between the tip and the material topography as well as a finite interaction volume caused by the spreading of the current from the tip [22]. We have also used the NIST SRM 3451 reference materials to demonstrate repeatability and reproducibility of the nanoscale resistance measurement on thermoelectric materials. The sample is a Bi2Te3 polycrystalline materials. A typical topography and resistance scan is shown in Fig. 25.

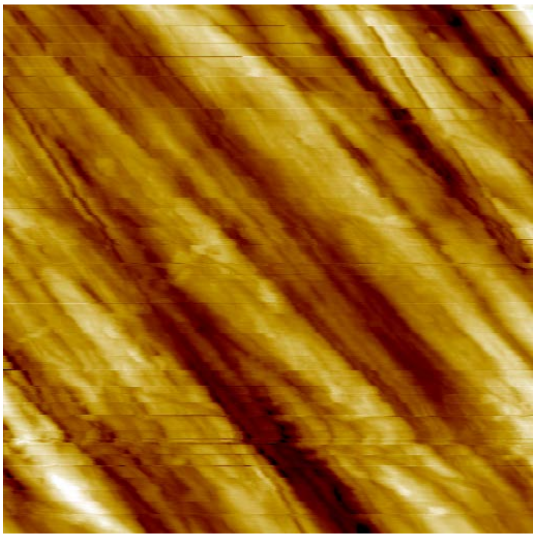

Fig. 25a. Topography scan 10 x 10 μm, z range 50 nm

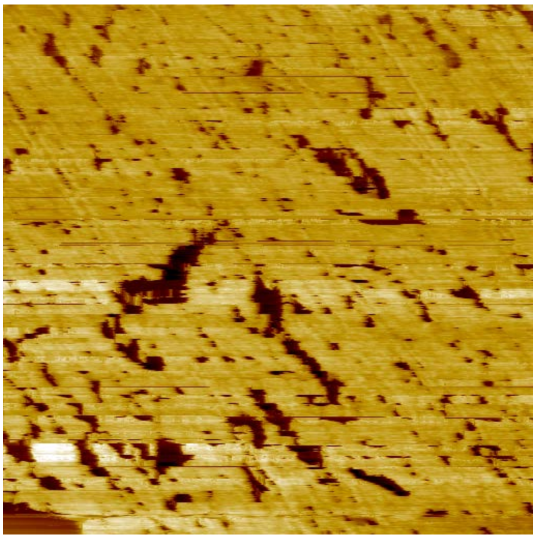

Fig. 25b. Resistance scan, z range kΩ to MΩ

A typical I-V curve average over ten points on the sample is shown in Fig. 26.

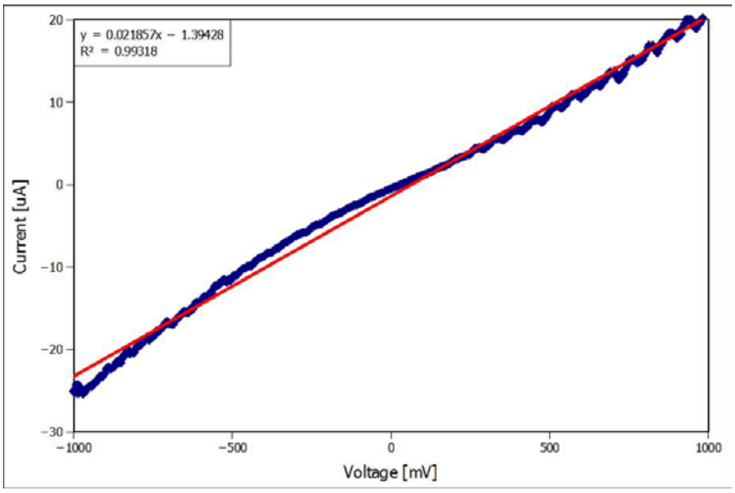

Fig. 26. Average of 10 I-V curves on the most conductive part of the NIST samples and a linear-fit showing a total resistance of 45 kOhm

The total contribution of the AFM cantilever and the AFM set-up resistance was measured using a pure copper disk with the oxide layer removed using deoxit[tm] .The force applied to the sample was changed accordingly to try to have the same contact area as with our measurement. Measurements indicate a consistent value of 21+- 2 kOhm with a heavily doped diamond doped cantilevers; note that this value will depend strongly on the resistance of the cantilever used.

The tip radius and probe-sample interaction area can also be determined using contact models and by performing force-distance curve measurements in every pixel of the image. This allows the mechanical and geometric properties of the probe-sample contact to be determined. CMI has created a set of tools for treating force volume data in Gwyddion: force-distance curves determined in every pixel can thus be evaluated automatically as shown in Fig. 27.

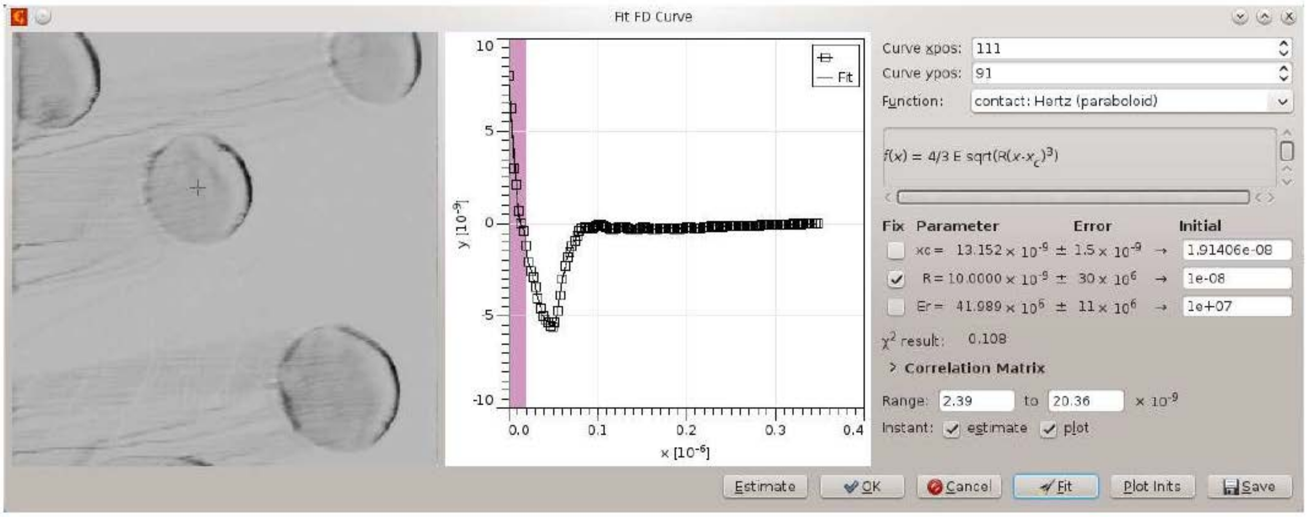

Fig. 27. automatic force-distance fitting module user interface

3.3.3 ***Nanoscale Thermal Conductance Measurement***

To measure thermal conductance, we have developped a technique using scanning thermal microscopy cantilever. By applying a large current (1 mA) into a nanoscale electrodes patterned on the cantilever, we can heat the probe while in non-contact. The temperature of the probe can be calibrated by contacting a thermal stage and by measuring the variation of resistance in the probe, which is highly temperature dependant. When the probe is in contact with a material under test at room-temperature, a new heat dissipation channel through the sample thermal conductivity is created; we can then measure the additional electrical power required by the probe to keep the probe temperature (or resistance) constant.

All lateral resolutions were computed following the ISO draft standard ISO/TC 201/SC 9 N168. The precision was approx. 6 % for materials with low thermal conductivity ($\lambda < 3$ W/Km), which represents the range of thermal conductivity for most current thermoelectric materials.

A typical thermal resistance map is shown in Fig. 28. Note that due to a software feature of the AFM, there is a build-in factor of 50 between the current displayed in the software and the real current put through the probe.

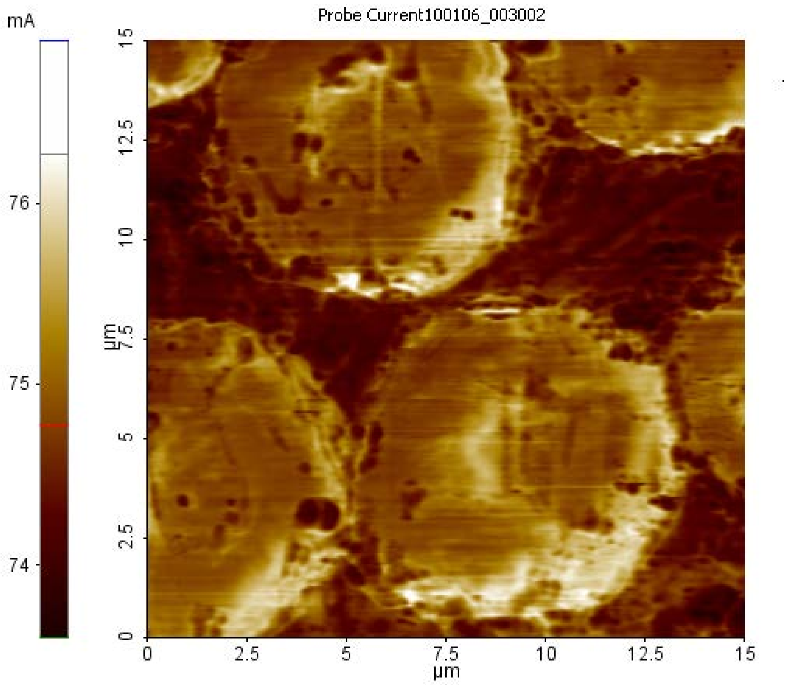

Fig 28. Thermal conductivity measurement on commercial test sample

To demonstrate the precision of the method, a series of twelve measurements were made on the same material. The additional current, which is proportional to the power dissipated by thermal conductivity through the sample was measured (Fig. 29).

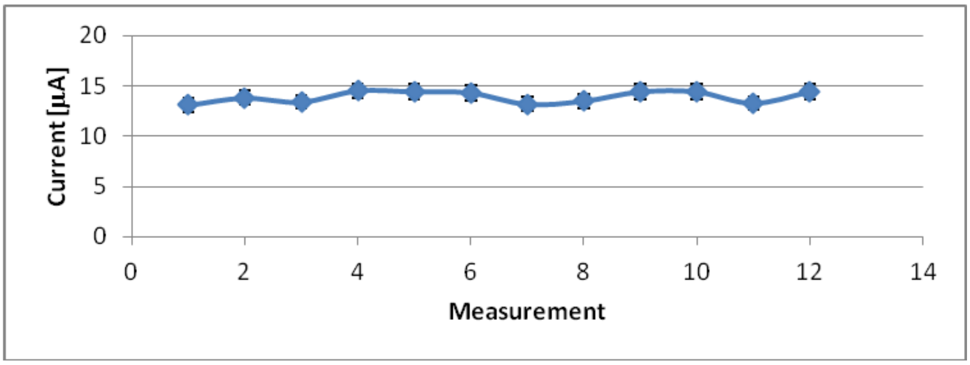

Fig 29. Average additional current required when in contact with identical materials (epoxy) at a constant voltage of 5 V

3.3.4 ***Nanoscale Seebeck Coefficient Measurement***

We have demonstrated for the first time Seebeck coefficient measurement with a lateral resolution better than 100 nm. This was done by measuring voltage change vs temperature change between a cold AFM cantilever (Room temperature) and hot sample (Fig. 30). All thermopower data was precise to 10 % and able to differentiate between n- and p-type materials. The technique is sensitive enough to be able to image small potential differences between single material grains; however, we were not able to exclude topographical artefacts.

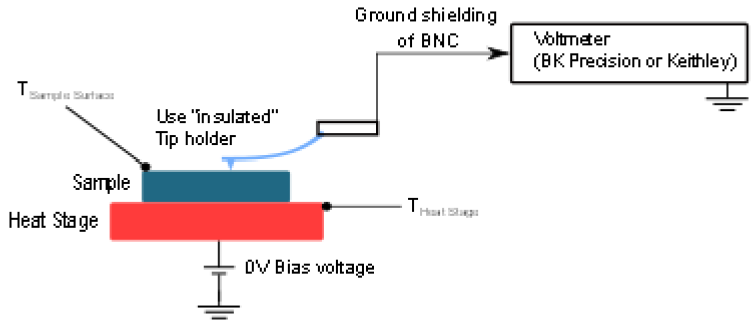

Fig. 30. Connection diagram for point contact measurements

To quantify the accuracy and precision of the method (Fig. 31), we had to use a micro-structured Bi2Te3 reference material (n- type) from NIST. This was due to the difficulty to polish other reference materials and sensitivity to type of dopant was demonstrated with a p- type sample form the British company "European Thermodynamics" also based on Bi2Te3.

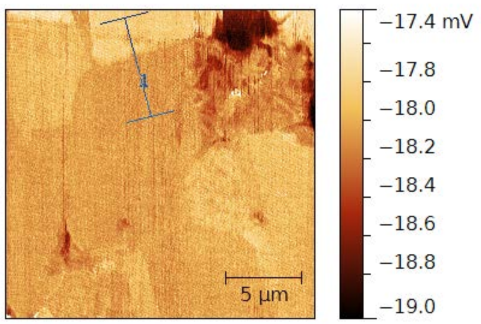

Fig. 31. Scan of NIST sample with newly develpoed thermopower AFM technique. Line indicates position of the section

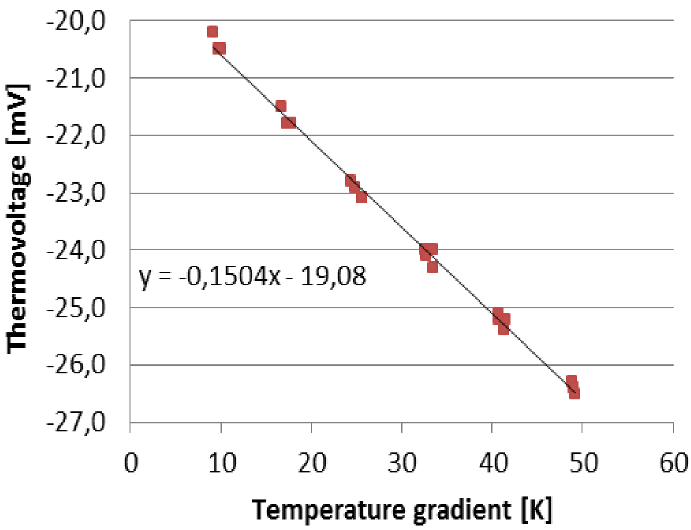

The average deviation from the accepted reference value was 35 %. While the measurement accuracy is poor, the precision of ~10 % offers great hopes to develop the technique to explore nanoscale variation of thermoelectric materials properties. CMI also contributed a model of thermal resistance of the tip with the sample, PTB and CMI provided reference materials and data.

3.3.5 *Section Summary*

This section demonstrates the development of measurement techniques for the characterisation of thermal energy transduction at the nano- scale (part of Objective 4). A key outcome was that, while conductance measurements at the nanoscale were usually reliable, conductivity measurement depends critically on:

1. the exact value of the contact area between the tip and the surface and
2. the transport model (classical or ballistic) used.

Unfortunately, AFM is right in the range where both mechanisms will contribute, depending on the exact value of the mean-free path value - for the phonons or the electrons. Therefore, a reliable value for thermal or electrical conductivity at the nanoscale cannot therefore yet be trusted from these measurements.

The project demonstrated for the first time nanoscale Seebeck coefficient measurement with a lateral resolution better than 100 nm.

3.4 Piezoelectric, Electrostatic and MEMS Energy Harvesting Metrology

3.4.1 *Section Introduction*

This section presents the development of methods for specifying and measuring performance parameters (efficiency, power, power density) for electro-mechanical energy harvesting as part of Objective 1. It also presents results relating to measurement at micro and nano-scales for electro-mechanical energy harvesters using piezoelectric, electrostatic and MEMS technologies, relating to Objective 4 (nanoscale measurements for thermoelectric harvesting were presented in section 3.3).

Section 3.4.2 describes research into the characterisation of electrostatic MEMS devices. Section 3.4.3 describes generic methods of measurement of macroscopic vibration harvesters. Energy harvester performance depends on vibration amplitude, frequency and the electrical load. Behaviour can be complex including non-linear effects that are not easily described by measurements under a single set of conditions. New facilities have therefore been developed for parametric mapping of energy harvester performance as a function of amplitude, frequency and electrical load. Methods of measurement of conversion efficiency were also shown, building on the work described in Section 3.2. These methods were applied here to piezoelectric harvesters, but could be used for most types of inertial type vibration harvester. Novel results were shown on losses in piezoelectric cantilevers. Section 3.4.4 presents new approaches to the measurement of energy harvesting and electro-mechanical energy conversion at the micro and nanoscales.

3.4.2 *Electrostatic MEMS Characterisation*

A common method for harvesting from vibration is to use a resonant mass-spring structure where the extension of the spring creates strain or displacement in a piezoelectric material. In general, the energy harvesting performance will be highly dependent on the frequency, amplitude and load, and all of these factors need to be considered in the valuation of energy harvester performance. However, there is an additional complication with active materials in that the electrical load can affect the stiffness of the system and non-linear effects can change the resonant frequency. For measurement of efficiency, it is also necessary to measure mechanical force or energy. At a macro-scale the measurement issues relate to providing facilities capable of exploring this complex multi-parameter space, and or providing reliable measurements of efficiency, over a sufficiently wide range of the parameters. At smaller length scales special techniques are required to measure the resonant properties of MEMS devices, and their energy harvesting performance. At even smaller length scales there is significant interest in nano-structured materials for electromechanical energy conversion, and techniques are required for evaluation of performance when built into a macro-scale device as well as energy coupling at the micro- and nano- scales. This section presents research results on facilities and techniques developed for the measurement of resonant behaviour of MEMS devices, electromechanical and piezoelectric conversion from macro-to nano-scale and magnetoelastic energy conversion.

To go with their successful deployment, MEMS sensors in general require a source of energy of reduced dimensions as MEMS-based vibrations powered energy harvesters have a power rating in the nano to milli watts range. Whatever the type of mechanically powered energy scavengers, electrostatic, electromagnetic or piezoelectric, the maximum electrical power generation from mechanical vibrations of MEMS transducers is given at resonant frequency, particularly when the source amplitude is small compared to the possible proof mass displacement and has only a narrow frequency bandwidth. Hence, knowledge of the resonant frequency and the damping factor of MEMS-based generators is crucial for matching them to the vibrational sources specifications.

To measure resonant frequency of MEMS actuators, different methods are available ranging from blur-envelop techniques and viscous damped measurements to sophisticated electronic measurements. LNE proposed a new harmonic distortion technique to measure resonant frequency by using the mechanical-electrical analogy of MEMS variable capacitor acting as a low-pass filter. This allowed us to have access to both resonant frequency and damping factor of the mechanical system through the determination of the filter parameters by sampling techniques. This method differed from existing ones as it could be applied to MEMS embedded systems where only electrical measurements were allowed, to devices with high Q factor (ratio of the resonance frequency over the full width at half-maximum bandwidth of the resonance) where classical methods lack accuracy and even to very damped MEMS that do not display any resonance behavior.

The electrical power generation from mechanical vibrations in almost all energy harvesters is achieved through a mechanical resonator made of a proof mass m coupled with the environmental vibrations by an elastic spring having a stiffness k (Fig.32). Thanks to this coupling, the mass oscillates in the reference system and accumulates a mechanical energy, which is converted into electric energy through an electromechanical transducer. The damping factor α has two components: one related to the inertia of the mass, which corresponds to the energy losses and the second is related to the force induced by the electromechanical transduction.

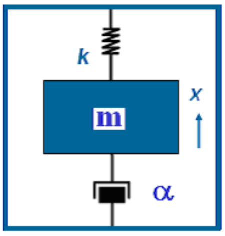

Fig. 32. Schematic representation of a vibrational energy harvester.

The electrostatic resonant energy harvester includes a mechanical resonator associated with a capacitive transducer. The capacitive transducer is a device with two electrodes; the first one is attached to the proof mass, the second electrode is being fixed to the frame and submitted to the external vibrations. To characterise the dynamical mode motion of the capacitive transducer, an alternating electrical voltage is applied to the MEMS variable capacitor. Under an applied voltage bias, the MEMS capacitance varies with the displacement *x* as:

$$C(x) = \frac{C_0}{1 - x}$$

where C_0 is the capacitance at rest. If the frequency of the applied voltage is very low compared to the resonant frequency, the displacement can be considered as being instantaneous. If it is very high, the dynamic displacement can be neglected and the RMS voltage is only taken into account, which also causes a static displacement. Hence, in the dynamic mode, the overall system mass + spring + damper is equivalent to a low-pass filter which will be characterised by its cut-off frequency and its damping factor. It can be modelled by an electrical LC filter damped by a resistor. Starting from the applied voltage $v(t)$, the electrical force $f(t)$, the displacement $x(t)$, the capacitance $c(t)$ and at last the current $i(t)$ were determined. The relation between $i(t)$ and $v(t)$ completely defines the electrical characteristics of the dipole.

Using *Genesys*™ software, we built an electrical model of this non linear-capacitance $C(x)$ allowing the definition of the relationship between current and voltage at any times. The equations defining the current as a function of voltage and time are represented in the flowchart in fig 33, where V_{pi} refers to the pull-in voltage of the MEMS (the DC voltage beyond which the two electrodes of the variable capacitor were brought instantaneously together). Mechanical stoppers were also used in the system to avoid an unwanted electrical contact of electrodes.

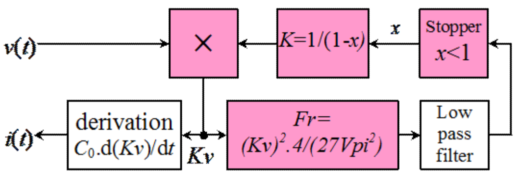

Fig. 33. Flowchart of fundamental equations of the MEMS

To perform the calculations, the MEMS variable capacitor was wired as a feedback element on an inverting operational amplifier and then driven by a sine current. The pull-in voltage is set at 5 V and the resonant frequency at 10 kHz. Fig 34 shows the RMS voltages of harmonics, H1 being the fundamental signal. Before the stopper, only the 3rd harmonic (H3) is present.

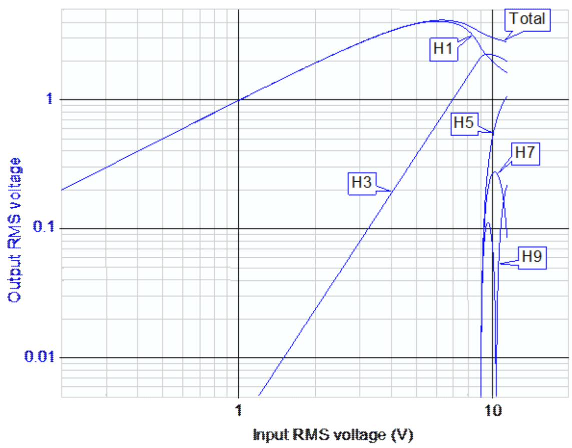

Fig. 34. Calculations of RMS voltages of harmonics of a MEMS variable capacitor

When varying the frequency of the bias voltage, the displacement *x* is filtered by the mechanical low-pass filter, and the distortion follows the response curve of this filter. The frequency of the mechanical vibration is twice the electrical signal frequency. Fig. 35 gives a MEMS device with a resonant frequency of 10 kHz the RMS voltage of the 3rd harmonic (0 dB is the *V*pi reference). Seven curves were plotted for each input voltage, with the damping factor α varying from 1/8 up to 1 with √2 ratios. In all cases, the cut-off frequency is 5 kHz. This shows that in theory it is possible to determine the mechanical parameters (cut-off or resonance frequency and damping) by measuring this 3rd harmonic distortion.

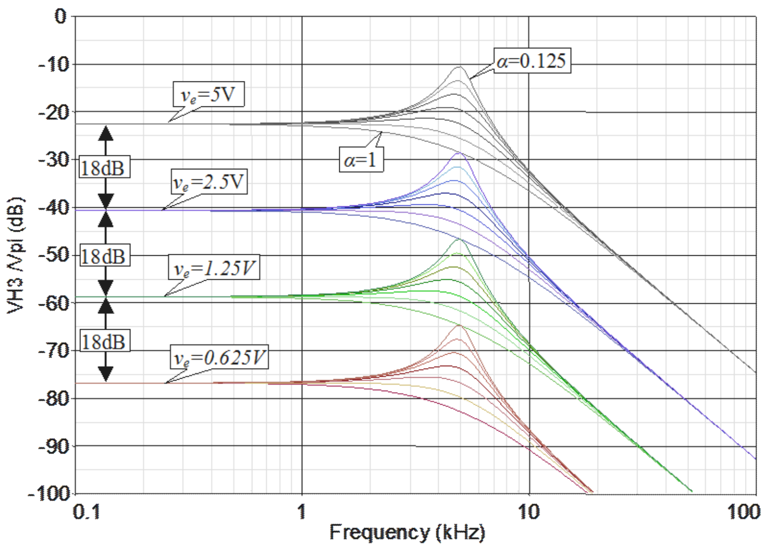

Fig. 35. Absolute level of the 3rd harmonic with sine current input

Several variable capacitor MEMS, named B1, B2 and B3, were designed at LNE using CoventorWare software [5]. The structures were made of fixed and movable electrodes fitted with split-fingers, which defined the gap of the variable capacitor (Fig. 36). Spring dimensions (length and width) were calculated to have a stress below 1 GPa with a displacement equal to one third of the gap. Table 1 gives an example of the various dimensions of a typical MEMS structure B1 designed to have a resonant frequency of 0.8 kHz (B2 and B3 MEMS structures have calculated resonant frequencies of 2 kHz and 4 kHz respectively).

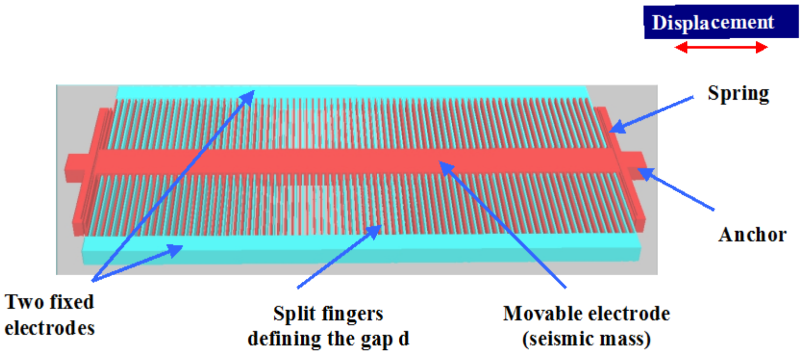

Fig. 36. Structure design of the split-fingers MEMS

Table 1. Dimension (in μm) of a MEMS structure B1 having a resonant frequency of 0.8 kHz.

Gap		4
Movable mass	Length	1292
	Width	150
Fingers	Number	150
	Length	350
	Width	6
Spring	Number	4
	Length	265
	Width	4

For the fabrication of the MEMS stuctures, we used a SOI surface micromachining process available at Tronics Microsystems as aMulti Project Wafer (MPW) process [6]. It's based on a SOI wafer having the following dimensions: 60 µm for the active silicon layer, 2 µm for the silicon dioxide and 450 µm for the silicon wafer. The process (Fig. 37) starts with the etching of the electrodes, the springs and anchors, then the deposit of gold contacts, and a selective etching of the silicon dioxide to release the movable parts.

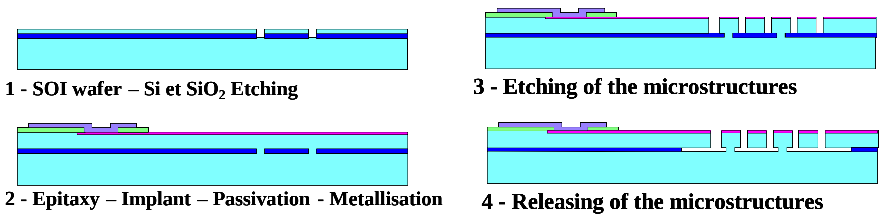

Fig. 37. Process flow of SOI surface micromachining process of Tronic

The final structure is composed by the SOI wafer containing the MEMS and a Si wafer acting as a cap for the protection of the devices (Fig. 38). This packaging can be hermetic in vacuum or not hermetic. Fig. 39 shows SEM photography of a MEMS device realised by this SOI surface micromachining process.

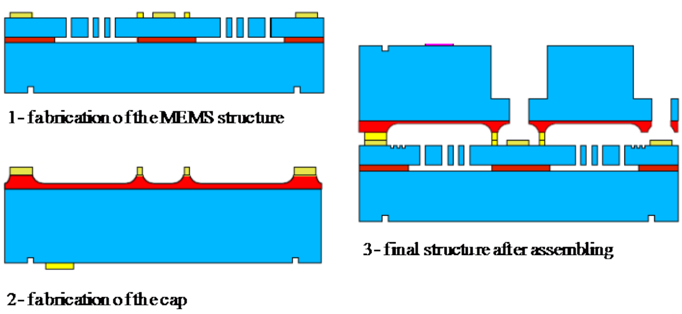

Fig. 38. Packaging process of Tronic

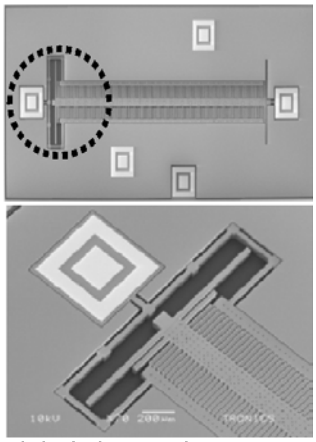

Fig.39. SEM of a MEMS structure: a global view and a zoom around the left side of the structure.

A Deep Level Transient Spectroscopy (DLTS) measurement system was used to measure the capacitance change with time when an impulse DC voltage is applied to the MEMS based electrostatic energy harvesters and to analyse the dynamic behavior of the movable electrode. Even if this system is used for semiconductors characterisations, it allows us to have information on the mechanical behavior of microsystems such as mechanical time responses, damping or resonance frequencies. The results also provide a comparison with the measurements carried out with the harmonic distortion set-up.

The resonant frequencies of the MEMS structures were measured according to different parameters e.g. voltage impulse and pressure. Fig. 40 shows the results of capacitance measurements carried out on B1 device where the voltage impulse varies from 0.5 - 1.5 V and for two pressure values (1 atm and 0.3 mbar). From these curves, the corresponding resonant frequencies were determined and shown in table 2.

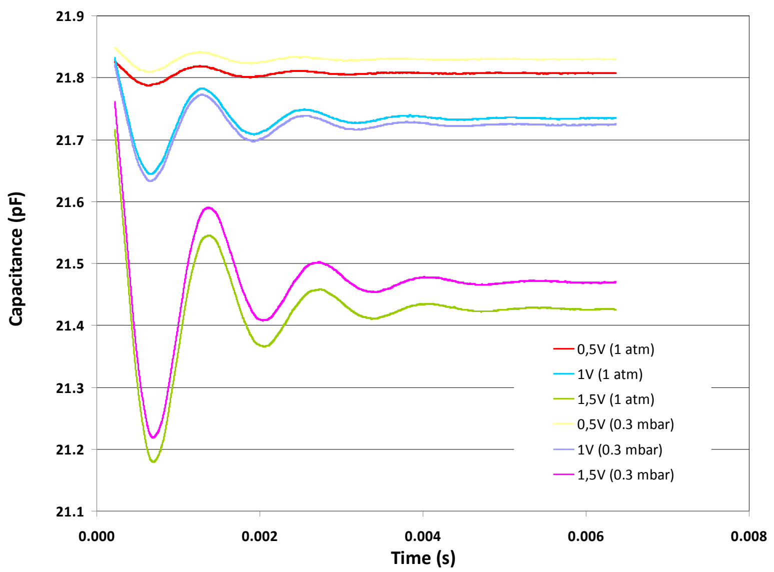

Fig.40 DLTS measurements of B1 (0.8 kHz) device for different voltage impulses and pressures.

Table 2. Resonant frequencies of B1 device determined from figure 9 measurements

Impulse voltage (V)	Resonant frequency (Hz)	
	1 atm	*0.3 mbar*
0.5	815	838
1	782	791
1.5	741	745

The measured resonant frequency depends on the values of the voltage impulse and the pressure under which the measurements were carried out: the frequency decreases when both voltage impulse and pressure increase: when the DC voltage applied to the electrodes becomes higher, the effect of the damping on the movable electrode is stronger and then the measured resonant frequency is lower. The same case happens when the pressure decreases: here the measured resonant frequency approaches the theoretical limit under vacuum of $\sqrt{k/m}$, which is the highest value for the mechanical resonant frequency of the system.

The results of DLTS measurements for the three electrostatic energy harvesters are shown in table 3. The reproducibility of these measurements was estimated to be of 5 parts in 10^3:

Table 3. Resonant frequencies of the MEMS devices determined from DLTS measurements

MEMS	Impulse voltage (V)	Resonant frequency (Hz)	
		1 atm	*0.3 mbar*
B1	0.5	815	838
B2	1	2276	2326
B3	2	4715	4832

We have shown that the mechanical parameters of an electrostatic actuated MEMS (cut-off or resonant frequency and damping factor) could be determined by the measurement of the distortion of the voltage across the MEMS capacitor when a sine current is flowing through it (the amplitude of the fundamental voltage is kept constant, *i.e.* the current is proportional to the frequency). Hence, we have implemented a measuring system of the harmonic distortion of the MEMS driven by a sine current. The input signal is provided by a SRS Stanford D360 having an ultra low distortion level and the output signal is sampled using either a digital voltmeter Agilent 3458A put in its subsampling mode or NI PXI-5922 sampler (Fig. 41). The spectrum of the signal is constructed through a FFT treatment (typically 1024 points and 16 points per period). The ratio H3/H1 is then measured over a wide range of frequency (Fig. 42), which allows us to determine the cut-off frequency (resonant frequency).

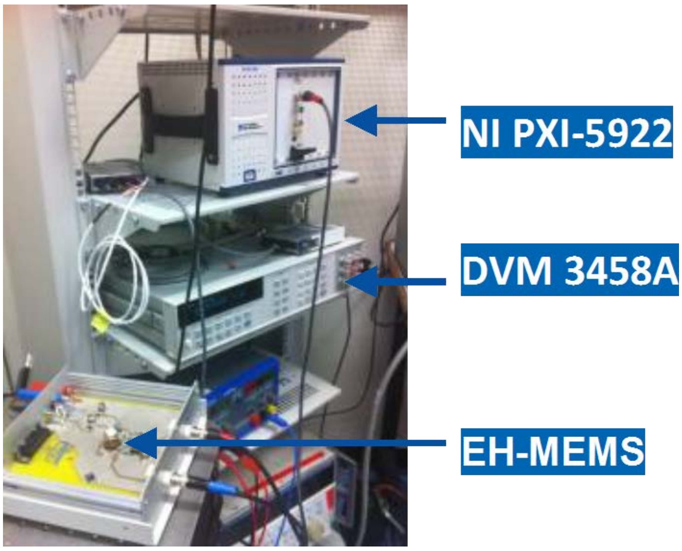

Fig. 41. Harmonic distortion set-up for resonant frequency measurement of MEMS devices.

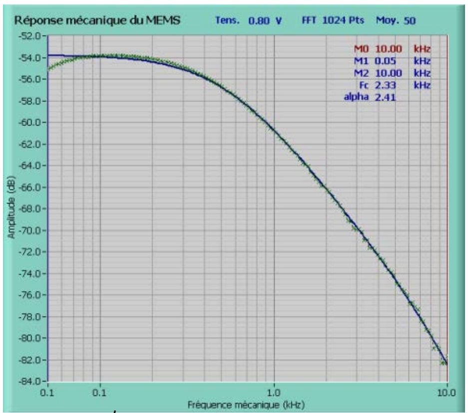

Fig. 42. Experimental curve showing the 3rd harmonic behavior versus the input current frequency and a theoretical fit allowing to determine the cut-off frequency and the damping factor

For all MEMS devices, the mechanical resonant frequencies were measured at ambient pressure and with a relative uncertainty of one part in 103 (1σ). This uncertainty was evaluated by a Monte-Carlo method applied on the curve fitting leading to the calculation of the resonant frequency. As shown in the table below, these results were in a very good agreement with the values estimated with DLTS measurements.

Table 4. Resonant frequencies of several comb-drive MEMS devices (B1 to B3) measured both by DLTS measurement system and the distortion technique

MEMS	**Resonant frequency (Hz)**	
	DLTS (σ=0.005)	*Distortion (σ=0.001)*
B1	815	823
B2	2276	2334
B3	4715	4754

LNE has also developed a new method for measuring mechanical properties of MEMS based harvesters, which uses the mechanical-electrical analogy of MEMS variable capacitor acting as a low-pass filter to give access to both resonant frequency and damping factor of the mechanical system through the determination of the filter parameters by sampling techniques. This method differs from existing ones as it can be applied to MEMS embedded systems where only electrical measurements were allowed, i.e. to high Q factor devices where classical methods lack of accuracy and even to damped MEMS that do not display any resonance behavior. In addition, this method of measuring mechanical quantities is based on the measurement of electrical quantities (voltage), allows us to ensure not only a best traceability of the measurements to the SI but also to reduce the measurement uncertainties as these electrical quantities were measured with high accuracy. Hence, uncertainties as low as 1 part in 103 were achieved for measuring resonant frequencies in the range of a few hundreds of Hz.

3.4.3 *Vibrational Energy Harvester Performance Mapping and Efficiency Measurement*

Facilities were set-up at NPL to perform sophisticated performance mapping of vibrational energy harvesters. Energy harvesting outputs depend on the amplitude and frequency of the vibration source as well as the load circuit. Fig. 43 shows the variation in power output of a piezoelectric device with frequency and acceleration. In many situations the power output does not scale linearly with vibration amplitude, so this kind of performance mapping provides important input into the development of standardised test methods and performance metrics.

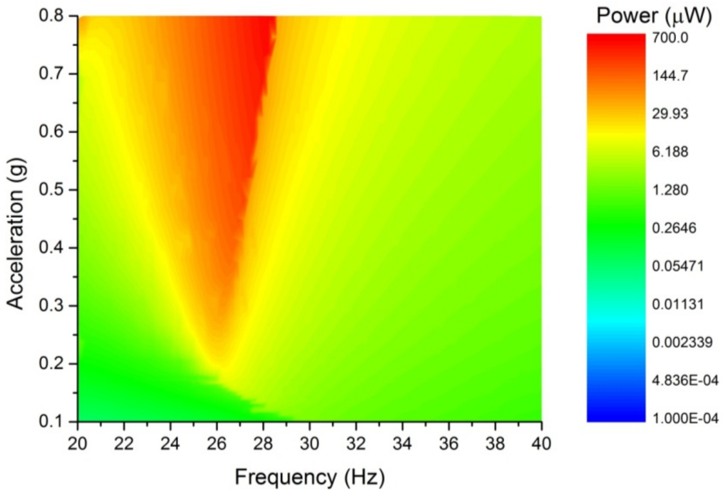

Fig. 43. Multi-variable performance mapping (frequency, amplitude, load).

For many vibrational harvesting applications, the energy harvester is much smaller than the source of the vibration e.g. a vehicle or piece of industrial machinery. However, in some cases we need to know the effect of the harvester on the vibration source e.g. human movement or mechanical frequency conversion methods for MEMS harvesters (in which case efficiency is an important parameter). In many situations losses can dominate performance and again, efficiency measurements can provide insight into these loss mechanisms. NPL and PTB collaborated in the development of methods for efficiency measurement. NPL developed facilities for the measurement of efficiency by two complementary methods (Fig. 44). Impulse excitation of the harvester and measurement of the subsequent decay in mechanical vibration and amplitude provides a simple method for efficiency measurement, particularly applicable to harvesters driven by impulses such as harvesters for heart pacemakers [23] or certain frequency converting MEMS devices.

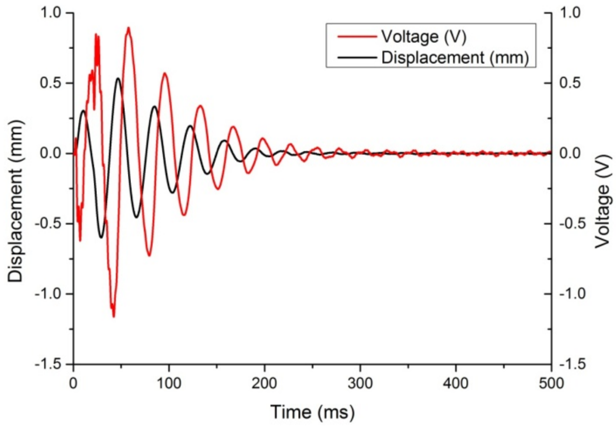

Fig. 44. Efficiency measurement using impulse and direct force methods illustrates source loading effect.

Direct measurements can be made by using a force sensor. The time-averaged mechanical power input is given by:

$$P_{mech} = \frac{1}{\tau}\int_0^{\tau} F \times v \, \mathrm{d}t = \frac{1}{2}F_0\, v_0\, Cos(\phi_v) = \frac{1}{2}F_0\, v_0\, Sin(\phi_d)$$

So measurement of force and velocity provides a measure of the input power which can be compared to the electrical power output to provide a measure of efficiency. This provides a more direct way of measuring the influence of the harvester on the vibration source e.g. a large phase shift between the force and the velocity is observed at resonance.

NPL developed a configurable piezoelectric cantilever to investigate internal losses in piezoelectric devices, showing that by reducing the piezoelectric coverage of the cantilever the energy output could actually be increased, with an optimum coverage of 2/3 for a rectangular beam with a tip mass.

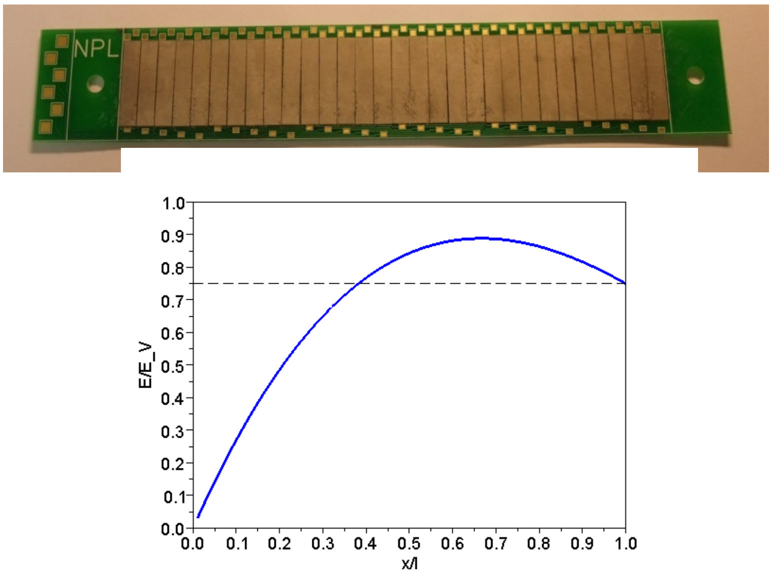

Fig. 45. Measurement of internal losses provides method for piezoelectric harvester optimisation [24]

3.4.4 *Micro- and Nano- scale electro-mechanical harvesting measurement*

MEMS technology is an important developing area for energy harvesting. NPL and LNE collaborated to develop a suite of measurement facilities to support the development of MEMS energy harvesters. Facilities were set-up at NPL for measuring MEMS harvester performance by integrating a miniaturised vibration source into a Laser Doppler Vibrometer scanning microscope (Fig. 46)

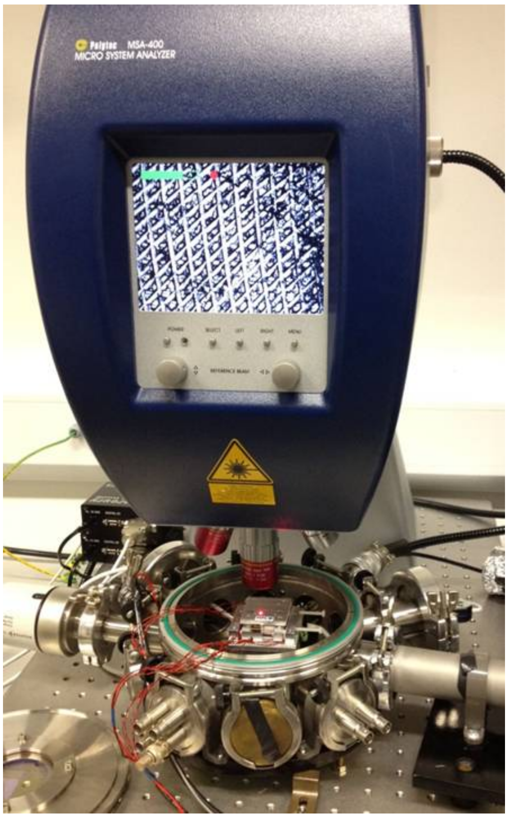

Fig. 46. facility for measuring MEMS vibration harvesters.

This provided the capability for measuring mechanical behaviour of the harvester under vibration. Measurements could be made in a controlled atmosphere or vacuum. As well as working with sample harvesters provided by stakeholders NPL and LNE collaborated to develop a range of test devices (Fig. 47).

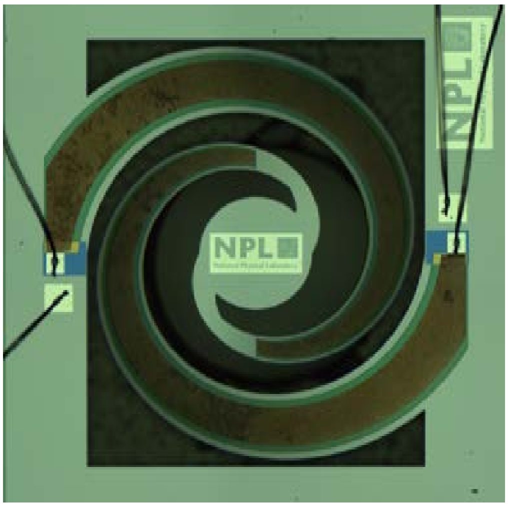

Fig. 47. piezoelectric MEMS energy harvester

NPL has also applied MEMS scale metrological tools to the measurement of piezoelectric properties at a scale compatible with MEMS energy harvesters (Fig. 48)

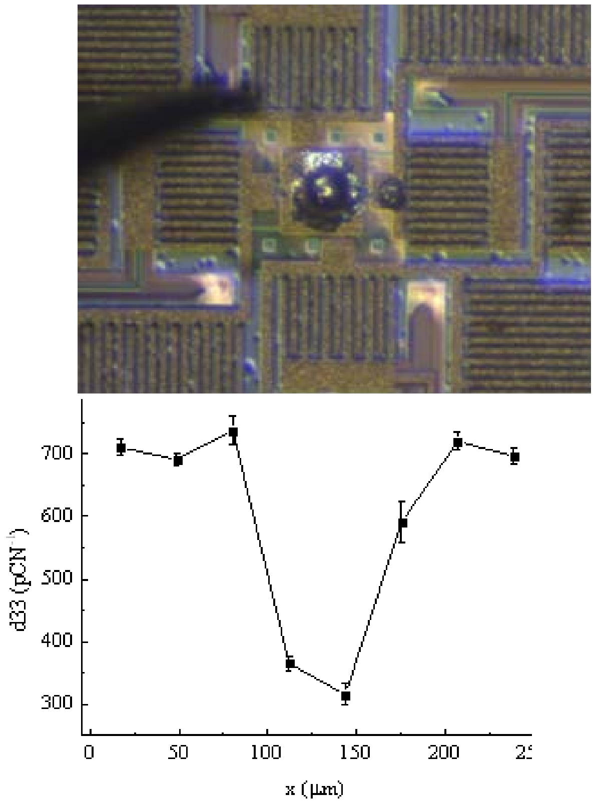

Fig. 48. MEMS Berlincourt system scanning a depoled region of a PZT ceramic.

Further down the length scale are piezoelectric nano-generators. Nanostructured piezoelectric materials can be fabricated by solution processing methods to provide potentially large area flexible harvesters. However, the lack of robust measurement techniques for this class of materials creates some uncertainty over their potential. NPL have developed (Fig. 49), a more robust approach to performance characterisation of nano-generators that takes into account the electrical load conditions and the mechanical source. This led to a 100 fold improvement in power output [25].

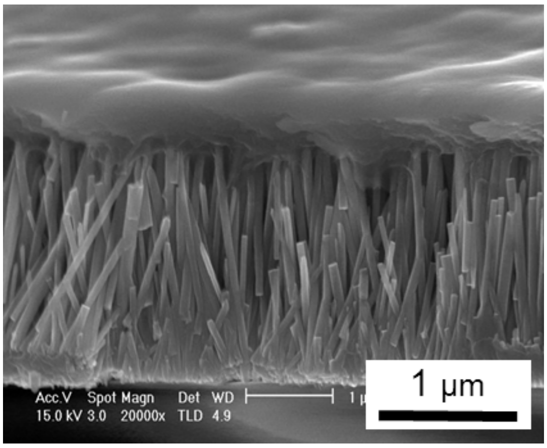

Fig. 49. Nano-structured Zinc Oxide energy harvester

In reducing length scales, energy coupling at the material level and its relationship to materials structure becomes important. To measure energy coupling at the nanoscale we applied piezo-response force microscopy (PFM) to measure the variation in energy coupling at the nanoscale and its relationship to the material structure (Fig. 50.8)

$d_{33} \times g_{33}$

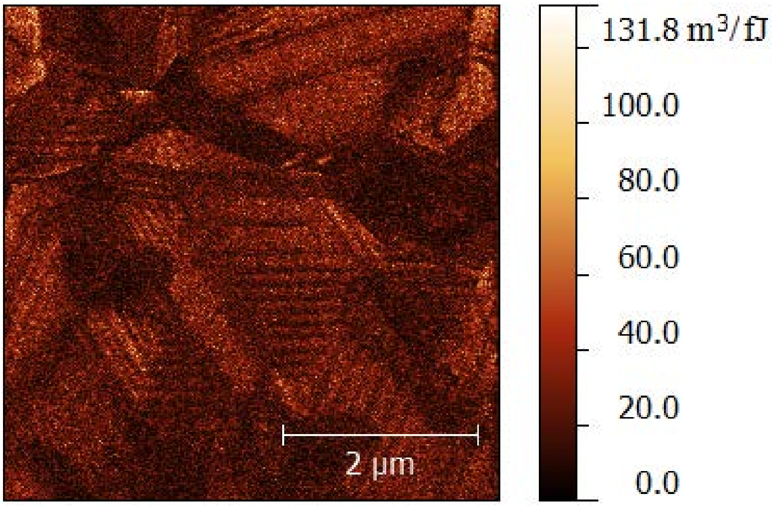

Maximum energy per cycle: $\frac{c}{ab}\, d_{33}\, g_{33}\, F^2$

Fig. 50. Measurement of energy coupling at the nanoscale

3.4.5 *Section Summary*

This section demonstrates the development of measurement techniques for the characterisation of electro-mechanical energy harvesters. To meet Objective 1, methods for specifying performance parameters (efficiency, power, power density) and their measurement, new capability was developed for the performance mapping of vibrational energy harvesters and applied to the characterisation of piezoelectric cantilever resonators. It was found that even at moderate vibration amplitude, significant effects of non-linearity were observed, resulting in appreciable shifts in resonant frequency with amplitude. This makes the currently widespread use of an acceleration normalised power density (typically measured in mW cm^{-3} m^{-2} s^{4}) as a figure of merit of questionable validity when measured at a fixed frequency. A solution is proposed whereby the measurement is taken across a range of frequencies to track the maximum power point. This performance mapping technique will provide important input into the development of standardised test methods and performance metrics.

Measurements of efficiency and losses in piezoelectric energy harvesters have shown that, in principle, efficiency can be high as, unlike thermoelectric generators, there is no thermodynamic limit. Efficiency is dictated by losses. A novel investigation of losses in piezoelectric cantilevers showed that there is an optimum coverage of piezoelectric material that maximises power output – less is more!

To meet Objective 4, measurement techniques for the characterisation of thermal and mechanical energy transduction at the micro- and nano- scales, for harvesting from mechanical sources, new techniques were developed for the measurement of energy harvesting and energy coupling at micro- and nano-scales. Measurements of the performance of nanostructured piezoelectric materials have, for the first time, brought a metrological perspective to this area which has supported rapid improvements in the performance of these materials.

3.5 Traceability for small non-sinusoidal signals

3.5.1 *Section Introduction*

The ability to traceably measure electrical power is central to the metrology of energy harvesting. This project developed new techniques for power measurement for the complex signals typically encountered in energy harvesting power measurements. These complex waveforms contain a wide range of frequencies, and to achieve accurate, traceable measurement requires detailed knowledge of the instrumentation characteristics.

This section describes the techniques developed for traceable measurement of small non-sinusoidal electrical signals for energy harvesters (Objective 3). To characterise uncertainties in the electrical measurement system and compare measurement techniques it is useful to have available synthetic waveforms with attributes typical of energy harvesting waveforms. Measurements made using both synthetic and real waveforms are described in this section. Section 3.5.2 describes candidate waveforms of interest for energy harvesting. Section 3.5.3 shows techniques for traceable electrical measurement using thermal converter techniques. Electrical sampling systems can be a considerable source of uncertainty in electrical quantity measurement. Uncertainties can be reduced for repetitive waveforms by averaging, but this is not possible for complex non-repetitive signals. Considerations relating to sampling techniques are described in Section 3.5.4. Sampling and thermal converter measurements are compared in section 3.5.5 and techniques are applied to real energy harvesters in Section 3.5.6.

3.5.2 *Electrical Waveforms*

The waveforms used for characterising EH devices should ideally come from characterising real harvester responses (e.g. characterised and generated). However, both samplers and TVCs can and should be traceably characterised, for well-defined waveforms. Sine waves are a clear contender but they lack any dynamic and spectral content except one clear and stable spectral line, which is obviously not the response expected form typical harvester. For using more complex signals, the following characteristics would be highly desirable:

1. Spectral bandwidth limited to the half of the sampling frequency
2. Multiple spectral lines or a spectral window covered by a signal
3. Relatively low signal amplitude / signal power ratio for TVC use
4. Repetitive signal with single steady state RMS amplitude

Three waveshapes were proposed (see Fig. 51):

1. Cosine shaped burst $U(t)=\mathrm{A}\cdot\left(0{,}5-0{,}5\cos(2\pi \mathrm{f}t)\right)\cdot\sin(2\pi N_B \mathrm{f}t)$
2. Raised cosine wave shape $U(t)=\mathrm{A}\cdot\frac{\mathrm{sinc}(\pi \mathrm{f}t)\cdot\cos(\pi\alpha \mathrm{f}t)}{1-(2\alpha \mathrm{f}t)^2}$
3. Damped oscillation $U(t)=\mathrm{A}\cdot\mathrm{e}^{-t/T}\sin(2\pi \mathrm{f}t)$

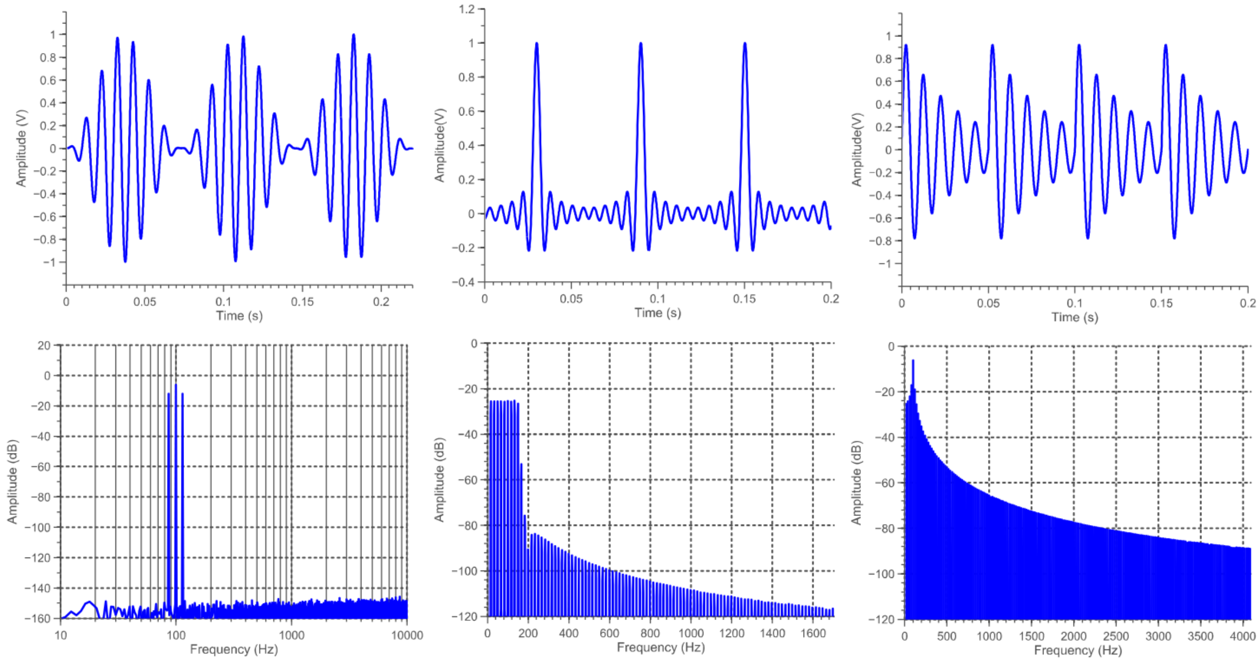

Fig. 51. Left: cosine shaped burst, mid: raised cosine, right: dumped oscillator. Below the amplitude spectra are shown. These signals allow for fairly clear calculation of power, frequency content and other useful information, which is necessary for demonstrating traceability for a complex signal.

3.5.3 *Traceability for electrical signals typical for microharvesters using thermal converters*

Development and construction of first prototype of arbitrary waveform generator with the following expected outputs: sinewave, triangular and square wave signal with precision frequency and amplitude setting, employing the 20-bit linear DA converter sampling at 1 MHz. The output amplitude scaling was found satisfactory for the direct use of thermal converters, covering measurements. This covers accurate scaling from 7 V down to 1 V. The self built generator was then compared with the commercial Agilent 33522A. Despite achieving better performance with self built device, there were still significant advantages on the commercial generator side as it seemed to fulfill all specifications and it was decided to use it – possibly with the added precision voltage buffer amplifier – for all measurements.

Thermal converters with dual heaters were designed and manufactured by modifying the existing layout. Supplying a variable DC voltage to the second heater in such away, that the output voltage (i.e. the operating point) is kept constant, allows to calculate the input power on the first heater by measuring the DC voltage on the second one without interrupting the input and switching to DC periodically as with conventional AC-DC transfer. Intensive modeling was performed and electronics for the controller were developed and built. Hard- and software to sample the DC voltage and calculating the input power was then set-up (Fig. 52).

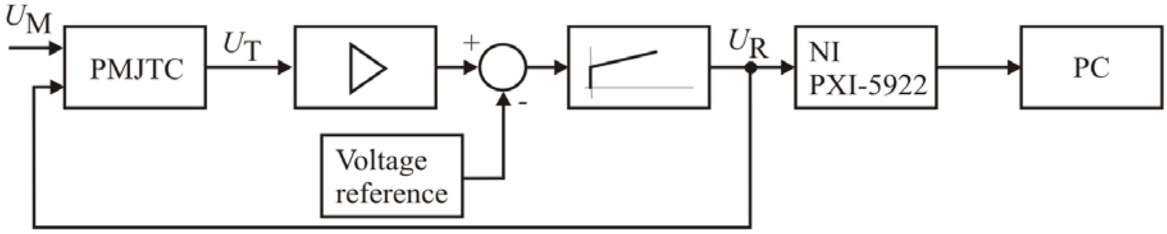

Fig. 52. Block diagram of the isothermal operation of a dual heater thermal converter

A second method to record the power and/or energy of impulse shaped input signals was developed (Fig. 53): The signal of interest is supplied to the heater of a thermal converter. The output voltage of this thermal converter is recorded as well as its ambient temperature. From the integrated output voltage and the rise of the ambient temperature, the energy content of the applied input pulse can be calculated, if the properties of the thermal converter are known.

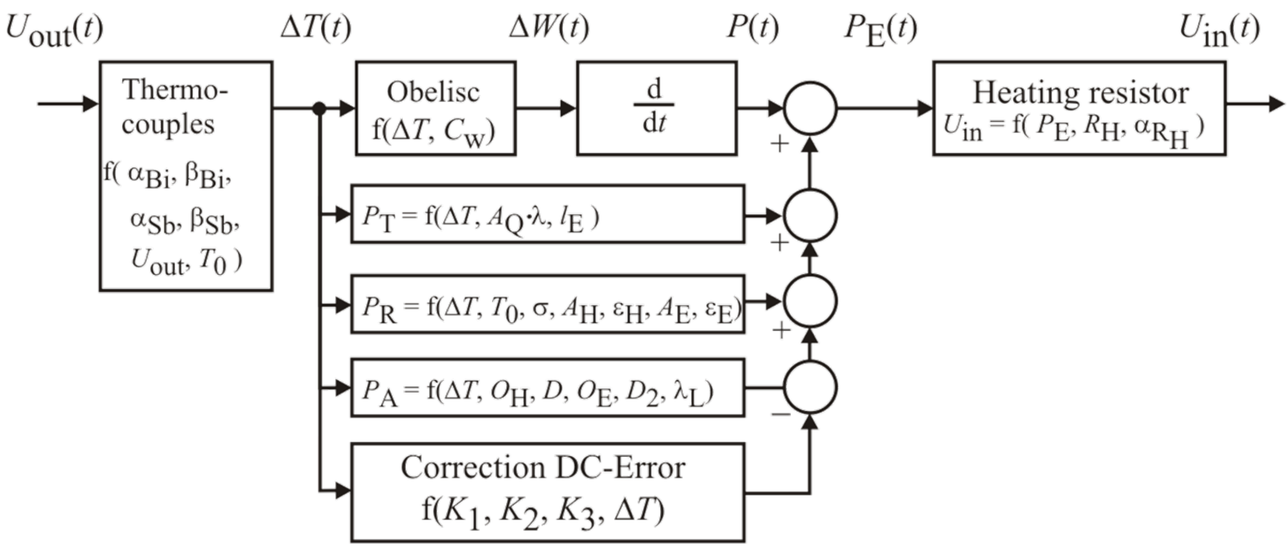

Fig. 53. Model of the thermal converter

The two systems were successfully verified by applying sinusoidal signals to determine their frequency response (Fig. 54) as well as DC pulses to check the measured power (Fig. 55).

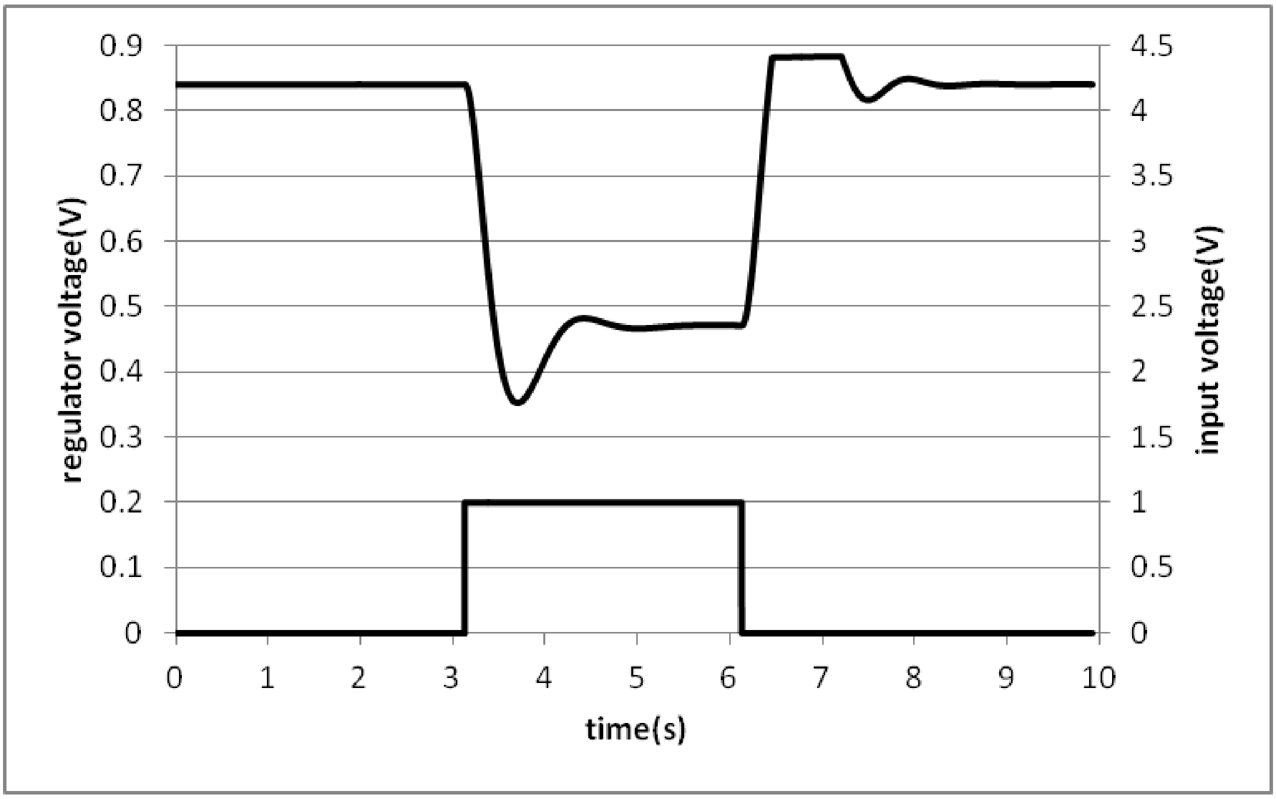

Fig. 54. Response to a rectangular input voltage pulse of the isothermally operated thermal converter

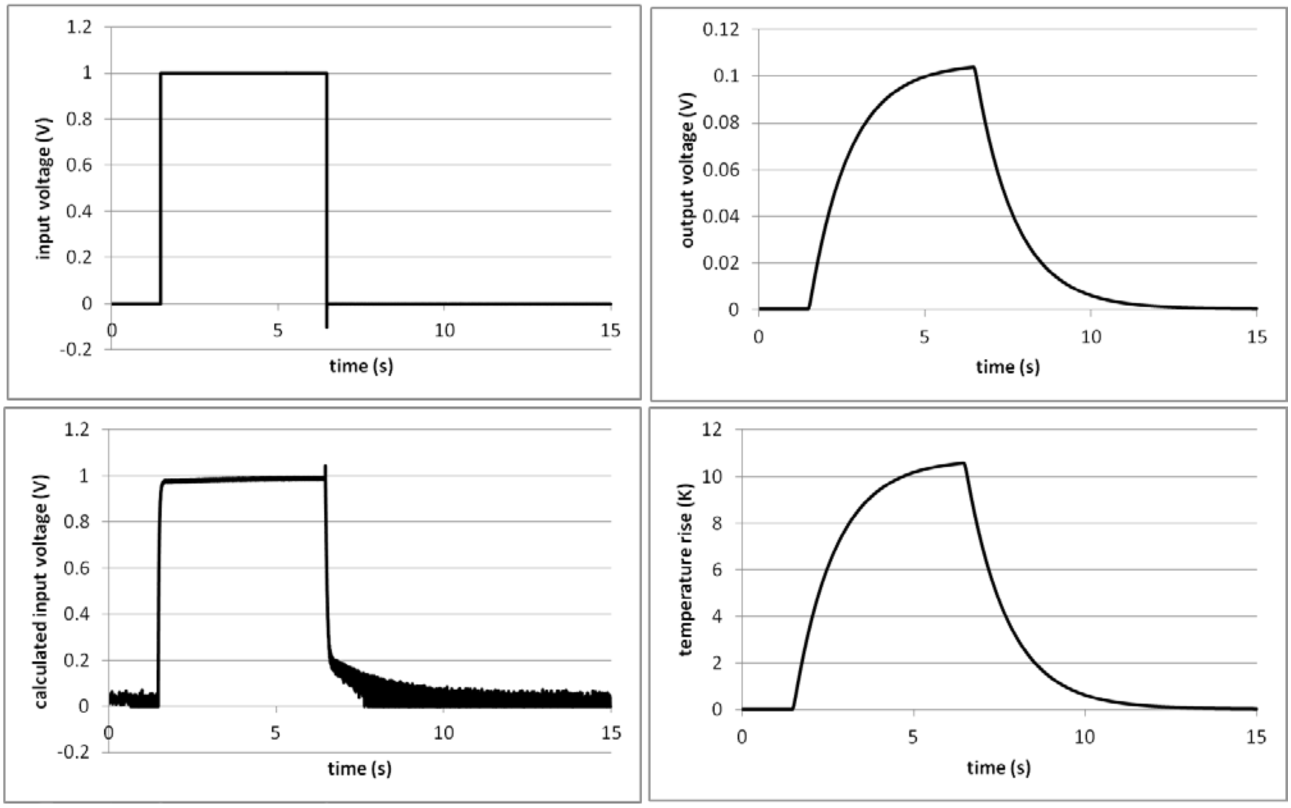

Fig. 55. Reconstructed rectangular input voltage pulse using the extended model of a thermal converter.

Amplifiers to be used with thermal converters were tested for key parameters as frequency response, dynamic range etc. and were traceably calibrated with sine waves. Amplifier front ends for digitisers were constructed and tested and the results were published at CPEM 2012 in Washington. For use in the intercomparisons, micro-potentiometers with different output voltages were built and characterised.

3.5.4 *Traceability for electrical signals typical for micr-oharvesters using sampling techniques*

INRIM developed a sampling system for the measurement of electrical signal from micro-harvesters. The sampling system was optimised for electromagnetic micro-harvesters, but can be extended to piezoelectric and electrostatic harvesters with suitable front-end amplifier.

The system is based on a commercial sampling board, National Instrument mod. PXI-4461 board, embedded in a PXI rack mod. 1036. The board has two synchronous-sampling ADCs, with five programmable input ranges (from 316 mV to 42 V full-scale). The measurements can be performed with input channels in differential DC coupling mode, with a 200 kHz sampling frequency, which achieves a Nyquist frequency of 100 kHz.

The sampling board is provided with two output DACs which are connected to a commercial shaker amplifier input, which permits mechanical excitation of the harvester being tested.

The acquisition is implemented with a Labwindows/CVI program that controls the PXI board, which permits to record batches of sampled points (up to 2^18 points per batch) with minimal dead time between batches. The program performed auto- and cross-correlation spectral densities of the channels. The program drives an output DAC with preloaded (sinewave, pulse, step, noise of different amplitudes) waveforms for mechanical excitation. Self- and external calibration of the board was also controlled by the acquistion program.

Data analysis was performed with a MATLAB program. The program allows the computation of a single-batch and averaged power and cross-power spectra and cross spectral densities, calculation of transfer functions, integration in the frequency domain of mechanical data (to compute velocity and position from measured acceleration).

The main contribution to measurement uncertainty is the temperature coefficient of the board, 85 ppm/°C. The contribution is reduced by performing measurements in a controlled temperature (0.5 °C) room.

PTB has set-up a dual channel sampling device equipped with a dual preamplifier and the combination of was characterised for DC linearity and the frequency response. The residual DC nonlinearity was found to be less than 100 µV in the full input range from -10 V to +10 V.

SIQ has developed a sampling system based on two Agilent 3458A sampling multimeters. The synchronised sampling techniques were evaluated with special emphasis on compensating for various errors, like aperture time error, input stage roll-off, and others. The system will provide for convenient sampling system, available for any metrology laboratory, with frequency coverage up to 50 kHz.

3.5.5 *Comparison of the two measurement systems using thermal converters and using sampling techniques*

The three waveshapes were used for the comparison (Fig. 56). A travelling standard was designed, built and characterised at PTB. Then it was successfully used in a bilateral comparison between PTB and SIQ, in January 2013. The standard allowed (for the first time) the simultaneous measurement of the same arbitrary signal with a thermal converter and with sampling devices.

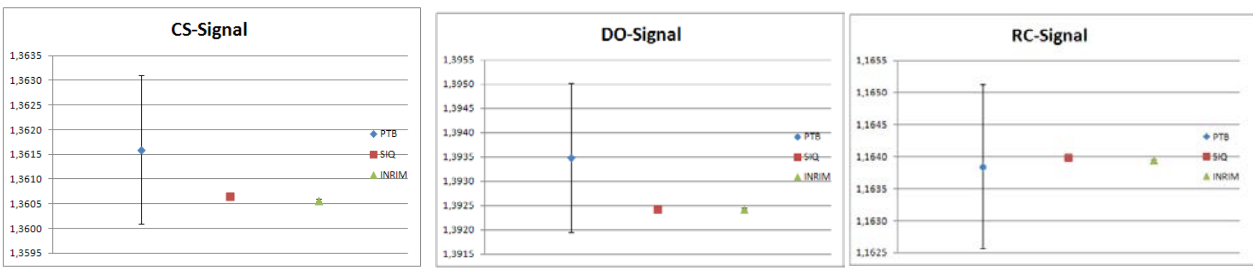

Fig. 56. *Results from the trilateral intercomparison between PTB, INRIM and SIQ at PTB in June 2013*

3.5.6 *"Real life" traceable characterisation of microharvesters*

The electromagnetic harvester developed by INRIM and the traceable sampling system were used to identify significant working parameters of the harvester. The most interesting parameter for sinusoidal excitation currently is the complex transfer function which links the voltage output to the input velocity (computed from measured acceleration). The real part of the transfer function is reasonably constant above a minimum excitation frequency. The imaginary part is linked to the reactive electromechanical energy.

Preliminary measurements of the electrical output power were performed by monitoring the voltage output when a calibrated resistive load was applied. A linear load permits a direct computation of the output power without the need for measuring the load current. The same measurement also allows the identification of the equivalent output impedance of the harvester. On the INRIM electromagnetic harvester, power output in excess of 0.1 mW was measured. The output impedance is essentially resistive and corresponds to the harvesting coil resistance.

A test bench for the characterisation of small energy harvesters, having a total weight lower than 100 g, was developed. The bench includes a shaker (The Modal Shop mod. K2007E01), acceleration measurement (PCB Piezotronics Model 355B03 accelerometer), force measurement (PCB Piezotronics Model 209C11). The test bench has since been used for the characterisation of an electromagnetic harvester and recently available electrostatic MEMS devices.

LNE developed a set of electrostatic MEMS harvesters for characterisation. Two measurement set-ups were developed for the purpose: C-V profiling measurement system, based on a commercial RLC bridge with DC bias voltage source, and electrostatic harvesters test bench which simulates harvester working conditions and measures the current output under dynamic periodical excitation. The newly assembled test bench at INRIM for the characterisation of mini- and microharvesters was used for characterisation measurements on electromagnetic (INRIM) and electrostatic MEMS (LNE) harvesters under controlled electrical load conditions. The feasibility of mechanical input power measurements, by using combined time-resolved measurements of force and acceleration, was investigated. Results of characterisation measurements of a new sampling system, based on Agilent commercial sampling board, toward improved traceability of electrical power measurements, were also made.

3.5.7 *Section Summary*

Systems for traceable measurements of complex electrical quantities typical of energy harvesting performance were developed, meeting Objective 4 of the project. Two methods were compared based on 1) thermal converter techniques and 2) sampling techniques. These techniques were assessed using both synthetic representative waveforms and real energy harvesters.

This project developed a new waveform generator that is able to precisely mimic over a million different waveforms or shapes (including non-sinusoidal) of the kind that are produced by energy harvesters. Because the properties of these simulated waveforms were already known, we were then able to use them to test and calibrate measurement equipment.

3.6 Summary of the research outputs

This project focused on the metrological aspects of thermal and electro-mechanical conversion methods in energy harvesting. It developed new measurement capabilities for key parameters in energy harvesting devices and then used them to increase understanding of the features and performance of energy harvesting devices. The new capabilities and increased understanding will contribute to the development of effective energy harvesting technologies.

For thermal converters, the technology of most interest, commercially and in research, is thermoelectric conversion. For electro-mechanical conversion, we adopted some generic approaches to measurement at different length-scales through the simultaneous characterisation of electrical and mechanical quantities. We also addressed technology-specific issues relating to energy converters that were of major interest commercially and under research, specifically piezoelectric, MST and electrostatic energy harvesters. Key project outputs were:

Performance mapping of vibrational energy harvesters (Objective 1)

Energy harvesting output depends on the amplitude and frequency of the vibration source as well as the load circuit. New facilities were developed to perform sophisticated performance mapping of vibrational energy harvesters with parametric variation of frequency, acceleration and load resistance. In many situations the power output does not scale linearly with vibration amplitude, so this kind of performance mapping will provide important input into the development of standardised test methods and performance metrics. Unique new facilities were also created for performance measurement of MST energy harvesting technology for applications such as power harvesting engine mounts.

New high temperature reference samples for thermoelectric converters (Objective 1)

The industrial realisation of accurate measurement of thermoelectric converter performance demands the availability of well-characterised reference materials. However, there is a lack of reference materials for the high temperature measurements required by the automotive industry one of the key early adopters of the technology. Two reference materials for Seebeck coefficients were characterised in the temperature range between 300 K and 650 K (Bi-PbTe) and between 300 K and 860 K (ISOTAN®). The relative measurement uncertainties ($k = 2$) obtained of the Seebeck coefficients were in the order of only a few percent, and it is the first time that reliable reference materials for Seebeck coefficients with low uncertainties at temperatures above approx. 400 K were made available.

Reduced uncertainties of measurement for thermoelectric converters (Objective 1)

Large uncertainties were associated with the measurement of thermoelectric harvesting, largely resulting from measurement of thermal properties, particularly at high temperature. New facilities were designed and constructed for measuring the thermal conductivity of thermoelectric materials from room temperature to 725 K resulting in reductions in relative measurement uncertainty to between 5 % and 8 % ($k=2$).

Efficiency measurement in vibrational energy harvesting (Objective 2)

For thermo-electric converters, efficiency is well defined (although difficult to measure). However, this is not true for electro-mechanical energy conversion, which requires a measurement of the mechanical energy input to a device as well as the electrical output. This project set-up unique facilities for the measurement of efficiency for electromechanical conversion, and developed models to predict efficiency in examples of commercial interest such as the piezoelectric cantilever. Efficiency is closely related to loss, and novel work within the project identified new sources of internal loss in piezoelectric converters, and demonstrated that power output can be significantly improved by reducing the amount of piezoelectric material, potentially saving cost as well as improving performance.

Traceable measurement of electrical quantities (Objective 3)

The ability to traceably measure electrical power is central to the metrology of energy harvesting. This project developed new techniques for power measurement for the complex signals typically encountered in energy harvesting power measurements. These complex waveforms contain a wide range of frequencies, and to achieve accurate, traceable measurement requires detailed knowledge of the instrumentation characteristics. This project developed a new waveform generator that is able to precisely mimic over a million different waveforms or shapes of the kind that were produced by energy harvesters. Because the properties of these simulated waveforms were already known, we were then able to use them to test and calibrate measurement equipment.

Energy harvesting at the micro- scale (Objective 4)

MEMS technology is an important developing area for energy harvesting. This project developed a suite of measurement facilities to support the development of MEMS energy harvesters. Energy conversion in MEMS devices is critically dependent on the often complex mechanical response to vibration, and damping from air movement and internal losses. This project developed a miniaturised vibration source integrated with a Laser Doppler Vibrometer scanning microscope to relate mechanical response at the micro-scale to power output for MEMS devices. A new technique was also developed for characterising the mechanical properties of MEMS harvesters by electrical measurements alone. Validation of measurement techniques requires performing measurements on well characterised devices, so piezoelectric and electrostatic MEMS samples were built to our own designs.

Energy conversion at the nano- scale (Objective 4)

Atomic-force microscope techniques were applied to the traceable measurement of energy coupling and electrical and thermal properties at the nanoscale. These techniques will pave the way for reliable measurement of energy conversion in emerging new nanostructured thermoelectric and piezoelectric energy harvesters.

4 Actual and potential impact

Dissemination:

- This research project has generated over 50 media articles in publications including the Smithsonian Magazine, Electronics Weekly, The Engineer, European Energy Review, Wind Energy Network, Pan-European Networks: Science & Technology, The Telegraph, as well as appearances and interviews on the BBC TV and the World Service radio. In addition 12 scientific papers listed in the table "List of the project's publications" at the end of this chapter.
- 11 editions of the "Metrology for Energy Harvesting" newsletter were published. Each issue includes project news and a "view from industry" interviews with industry leaders working in the field. The newsletter is circulated to the research project stakeholder group, and is also available to download from the research project website http://projects.npl.co.uk/energy_harvesting.
- The research project website http://projects.npl.co.uk/energy_harvesting provides access to research project information, issues of the quarterly newsletter and a research project blog / news section.
- An end of research project dissemination event provided an overview of the project achievements. More detailed coverage of the technical work was also presented in three workshops to an audience of industry and research organisations. The event was also webcast, and webcast recordings are available from the research project website http://projects.npl.co.uk/energy_harvesting.
- This project has produced 12 scientific publications in high profile jounals including Applied Physics Letters and Energy and Environmental Science.
- Our stakeholder list for the research project comprises over 100 contacts, 59 % are from industry and have benefitted from regular research project information through our newsletters and direct discussions with industry leaders.
- This research project has developed industrial training courses which were delivered in collaboration with IDTechEx as part of their Masterclass workshops at industry focussed conferences on energy harvesting and wireless sensors.
- NPL are represented on the UK's EPSRC Energy Harvesting Network, and presented this research project at events and workshops organised by the network.

Standards:

- NPL attended meetings of the ISA100.18 (International Society of Automation) power sources standards committee and presented this research project to the committee. Discussions were held with the chair of the committee, who has requested that NPL work with the committee on the development of standardisation of performance metrics and measurement techniques for this committee. It is envisaged that eventual adoption as an IEC standard would be sought.
- Discussions were held with the secretary of IEC/TC 113 'Nanotechnology standardisation for electrical and electronics products and systems' on the development of measurement standards of piezoelectric and thermoelectric energy harvesting and energy storage using nano-structured materials., identifying a potential need for nanoscale characterisation of functional properties.
- Discussions were held with the chair of IEC TC47 who have started developing energy harvesting standards, regarding representation of our energy harvesting work on this committee. We will seek to participate in future development of these standards.
- NPL contributed to the UK Knowledge Transfer Network (KTN) Energy Harvesting Special Interest Group report on standardisation activities in energy harvesting. This was published as an industry report available from the special interest group website.

Industrial Impact:

- Morgan Advanced Materials, a global materials engineering company, have supplied NPL with various components for characterisation. The resulting measurement data and analysis were supplied to Morgan. This will help Morgan to provide energy harvesting metrics which will enable their customers to assess how a device will perform in a given environment, or to compare with products from other manufacturers.

- The project has also worked with a FTSE 100 global engineering company to apply measurement facilities developed in this research project to energy harvesters under development by the company.
- Piezoselex "Piezoelectric Pair Materials for the Selective Exclusion of Workplace Noise" is a Research for SME's, European Seventh Framework project for the development of an improved device for the prevention of noise induced hearing loss. The innovative new solution allows for specific ranges of sound frequencies (i.e. those within the range of speech and alarms) to be heard whilst significantly reducing other potentially harmful noise based. NPL's input to the project was based, in part, on NPL capability developed under this research project.
- LNE has joined a national French industry consortium composed of Thales Systems Avionic, Dassault Systems and four SMEs with the aim to develop vibration energy harvesters to supply autonomous sensors for aircrafts monitoring. This industrial project (RECAP) started in 2013 will be spread over three years and will be focused on the commercialisation of vibration powered 3D integrated sensors.

Policy:

- The project has had input into UK funding policy through the Technology Strategy Board energy harvesting special interest group (SIG). NPL worked with the SIG on the writing of a number of industry reports covering standards, materials sustainability, new materials and rectification as well as attending and presenting at SIG workshops. These reports and workshops provide information to industry as well as informing the Technology Strategy Board on funding strategies.
- NPL are represented on the scientific board of the ZeroPower FP7 co-ordination activity whose mission is to develop a strategic research agenda for energy harvesting in low power, energy efficient ICT.
- This research project has had two articles published by Pan European Networks "Science & Technology" publication which provides information to policy makers in the European Commission as well as government agencies and departments across the continent of Europe.

Scientific impact:

Challenge 1. Generic challenges for energy harvesting metrology

Systems for traceable measurements of complex electrical quantities typical of energy harvesting performance heave been developed and compared based on thermal converter techniques sampling methods. These techniques were assessed using both synthetic representative waveforms and on real energy harvesters (Section 3.5). The project has also developed a new waveform generator that is able to precisely mimic over a million different waveforms or shapes of the kind that are produced by energy harvesters. Because the properties of these simulated waveforms were already known, we were then able to use them to test and calibrate measurement equipment.

Models were developed for the measurement of conversion efficiency in micro-generators and applied to piezoelectric energy harvesters, showing good agreement between theory and experiment (Section 3.1). This work has illustrated that efficiency is not always the best quantity for describing the effectiveness of a harvester in a particular application. In many cases power output under defined conditions is more appropriate. However, there are applications where the source energy is finite or not free, such as harvesting from human or vehicle power where careful consideration must be given to efficiency and its measurement.

Challenge 2. Metrology challenges relating to particular energy harvesting technologies.

Large uncertainties were associated with the measurement of thermoelectric harvesting, largely resulting from measurement of thermal properties, particularly at high temperature. New facilities were designed and constructed for measuring the thermal conductivity of thermoelectric materials from room temperature to

725 K resulting in reductions in relative measurement uncertainty to between 5 % and 8 % (k=2) (Section 3.2). The system at MIKES is based on the 3-omega method and was tested and validated with several dielectric, semiconductor and metal bulk samples from room temperature up to 725 K. This is supported by a new capability for measurement of thermal conductivity, electrical conductivity and Seebeck coefficient for thermoelectrics based on the van der Pauw method is demonstrated, providing measurements of the thermoelectric figure of merit up to 700 K.

The evaluation of the figure of merit by using undisputed reference materials with known thermoelectric properties is essential for industry to validate testing methods and to allow the reliable benchmarking of thermoelectric materials. As a product of this research, two reference materials (CuNi44Mn1 and PbTe) for the Seebeck coefficient are now available from PTB (Section 3.2). The thermoelectric characterisation of the first reference material CuNi44Mn1 (homogeneity and short term stability) was completed within the certification process according to the ISO Guide 35. The characterisation with respect to the long term stability of the reference material according to the ISO Guide 35 is under way. PTB has performed a single sample certification for the Seebeck coefficients of this semiconducting material. This was supplied instead of a complete certification of this reference material on basis of the ISO Guide 35. It is planned to conclude agreements with suppliers of devices for measuring Seebeck coefficients (for instance the Netzsch Group in Germany) to incorporate at least one certified sample of a reference material for Seebeck coefficients for the delivery and sale of such devices. This would allow the supplier but also the customers to test the conformity of their devices and measurements and to estimate their own measurement uncertainties.

Performance mapping of piezoelectric energy harvesters (Section 3.4) has demonstrated that even at moderate vibration amplitude, significant effects of non-linearity were observed, resulting in appreciable shifts in resonant frequency with amplitude. This makes the currently widespread use of an acceleration normalised power density as a figure of merit, of questionable validity when measured at a fixed frequency. A solution is therefore, proposed whereby the measurement is taken across a range of frequencies to track the maximum power point.

A novel investigation of losses in piezoelectric cantilevers showed that there is an optimum coverage of piezoelectric material that maximises power output – less is more! This work was published (“Charge redistribution in piezoelectric energy harvesters” Stewart, M.; Weaver, P. M. & Cain, M., Applied Physics Letters, 2012, 100, 073901) and has received 10 citations in just one year since publication.

Challenge 3. Micro- and Nano- scale energy harvesting metrology

Measurements of the performance of nanostructured piezoelectric materials (Section 3.4) have, for the first time, brought a metrological perspective to this area which has supported rapid improvements in the performance of these materials. This work was reported in high impact journals such as Energy and Environmental Science.

Nanoscale thermoelectric measureemnts (Section 3.3) have shown that, while conductance measurements are usually reliable, conductivity measurement depends critically on (1) the exact value of the contact area between the tip and the surface and (2) on the transport model (classical or ballistic) used. Converting conductance measurements into conductivity for either thermal or electrical quantities is still, therefore subject to significant uncertainties associated with the physical model.

We have demonstrated for the first time Seebeck coefficient measurement with a lateral resolution better than 100 nm.

LNE has developed a new technique based on harmonic distortion analysis to accurately measure mechanical properties of MEMS vibrational energy harvesters (Section 3.4). Uncertainties as low as 1 part in 10^3 were achieved with this technique in measuring resonant frequencies ranging from a few hundreds Hz to tens of kHz. LNE has also designed and fabricated electrostatic and piezo MEMS based energy harvesters. The electrostatic devices were used as test structures for the development of the harmonic distortion method while the piezo harvesters were designed to fit with automotive applications. A presentation of these achievements was given in November 2013 to Valeo company.

List of the project's publications

Author(s)	Title of article / paper	Title of journal	Date of publication, issue number, relevant page numbers	Institutes involved
Stewart, M.; Weaver, P. M. & Cain, M.	Charge redistribution in piezoelectric energy harvesters	Applied Physics Letters	2012, 100, 073901	NPL
J. de Boor, C. Stiewe, P. Ziolkowski, T. Dasgupta, G. Karpinski, E. Lenz, F.Edler, and E. Müller	High temperature measurement of the Seebeck coefficient and the electrical conductivity	Journal of Electronic Materials	2013, Vol. 42, doi:10.1007/s11664-012-2404-z, p. 1711	PTB
Mauro Zucca, Oriano Bottauscio	Hysteretic modeling of electrical micro-power generators based on Villari effect	IEEE Transactions on Magnetics	2012, Vol. 48, no. 11, pp. 3092-3095	INRIM
Briscoe, J.; Jalali, N.; Woolliams, P.; Stewart, M.; Weaver, P. M.; Cain, M. & Dunn, S.	Measurement techniques for piezoelectric nanogenerators	Energy Environ. Sci.	doi:10.1039/C3EE41889 H	NPL
M.Zucca, O. Bottauscio, C. Beatrice, F. Fiorillo	Modeling Amorphous Ribbons in Energy Harvesting Applications	IEEE Transactions on Magnetics	October 2011, n. 10, vol. 47, p. 4421-4424	INRIM
Briscoe, J.; Stewart, M.; Vopson, M.; Cain, M.; Weaver, P. M. & Dunn, S.	Nanostructured p-n Junctions for Kinetic-to-Electrical Energy Conversion	Advanced Energy Materials	2012, 2, 1261-1268	NPL
Ernst Lenz, Frank Edler, Sebastian Haupt, Pawel Ziolkowski, and Hans-Fridtjof Pernau	Traceable measurements of electrical conductivity and Seebeck coefficient of β-Fe0.95Co0.05Si2 and Ge in the temperature range from 300 K to 850 K	Phys. Stat. Sol (c)	2012, Vol. 9, Nr. 12, p. 2432-2435	PTB
E. Lenz, F. Edler, and P. Ziolkowski	Traceable thermoelectric measurements of seebeck coefficients in the temperature range from 300 K to 900 K	Int. Jour. of Thermophys.	DOI 10.1007/s10765-013-1516-x	PTB
Rado Lapuh	Ushering in new standards for energy harvesters	The Engineer	12th November 2012	SIQ
A. Bounouh and D. Bélières	Resonant frequency characterization of MEMS based energy harvesters by harmonic sampling analysis method	Measurement	52 (2014) pp. 71–76	LNE
Briscoe, J.; Jalali, N.; Woolliams, P.; Stewart, M.; Weaver, P. M.; Cain, M. & Dunn, S.	Measurement techniques for piezoelectric nanogenerators	Energy Environ. Sci.	doi:10.1039/C3EE41889 H	NPL
Bowen, C.; Kim, H.; Weaver, P. & Dunn, S.	"Piezoelectric and ferroelectric materials and structures for energy harvesting applications	Energy and Environmental Science	2014, 7, 25-44.	NPL

5 Website address and contact details

Research project website address

http://projects.npl.co.uk/energy_harvesting/

Contact details

Contact Type	comment	WP No	Organisation	Name	email
Technical contact	WP leader	1	PTB	Bernd Schumacher	Bernd.Schumacher@ptb.de
Technical contact	Scientist	1	PTB	Alan Šala	
Technical contact	WP leader	2	PTB	Frank Edler	Frank.Edler@ptb.de
Technical contact	WP leader	3	NPL	Alexandre Cuenat	alexandre.cuenat@npl.co.uk
Coordinator Deputy	WP leader	4	NPL	Paul Weaver	paul.weaver@npl.co.uk
Technical contact partly Coordinator Deputy	WP leader	5	PTB	Torsten Funck	Torsten.Funck@ptb.de
Technical contact	PhD student	5	PTB	Tobias Möhring	
Technical contact	WP leader	6	NPL	Paul Weaver	paul.weaver@npl.co.uk
Coordinator	WP leader	7	PTB	Jürgen Melcher	Juergen.Melcher@ptb.de

Work Packages (WP)

WP No	Work Package Name	Active JRP-Participants *(WP leader in bold)*
1	Conversion efficiency of microgenerators, converting thermal or mechanical energy into electrical energy	***PTB***, NPL, INRIM, LNE
2	Figure of merit of macroscopic thermoelectric reference materials	***PTB***, NPL, MIKES
3	Metrology for nanostructured thermoelectrics	PTB, ***NPL***, MIKES, CMI
4	Piezoelectric and magnetic materials for energy harvesting from macro to nano-scale devices	***NPL***, INRIM, LNE, CMI
5	Traceability for small non-sinusoidal signals	***PTB***, INRIM, SIQ
6	Creating Impact	***NPL*** and all
7	JRP Management and Coordination	***PTB*** and all

JRP-Partners:

	Participant Type	Short Name	Organisation legal full name	Country
1	Funded Partner	PTB	Physikalisch-Technische Bundesanstalt	Germany
2	Funded Partner	CMI	Cesky Metrologicky Institut Brno	Czech Republic
3	Funded Partner	INRIM	Istituto Nazionale di Ricerca Metrologica	Italy
4	Funded Partner	LNE	Laboratoire national de métrologie et d'essais	France
5	Funded Partner	MIKES	Mittatekniikan Keskus	Finland
6	Funded Partner	NPL	NPL Management Limited	United Kingdom
7	Funded Partner	SIQ	Slovenski Institut za Kakovost in Meroslovje	Slovenia

Project logo:

Metrology for
energy harvesting
European Metrology Research Programme

[1] http://www.euractiv.com/en/environment/batteries-directive/article-117445

[2] Directive 2006/66/Ec Of The European Parliament And Of The Council, Official Journal of the European Union, 2006L0066, 06.09.2006 (http://eur-lex.europa.eu/LexUriServ/LexUriServ.do?uri=CONSLEG:2006L0066:20081205:EN:PDF)

[3] Evaluation of measurement data — Guide to the expression of uncertainty in measurement (http://www.bipm.org/en/publications/guides/gum.html)

[4] C.B Williams, B. Yates, "Analysis of a micro-electric generator for Microsystems", Sensors und actuators, A52, pp. 8-11 (1996).

[5] S. Roundy, P. K. Wright, J. M. Rabaey, "A piezoelectric vibration based generator for wireless electronics", Smart materials and structures (13), pp. 1131-1142, 2004.

[6] A. Erturk, D. J. Inmann, A distributed parameter electromehanical model for cantilever piezoelectric energy harvesters, Journal of vibration and acoutics, vol. 130, August 2008b.

[7] Luigi Pinna, Ravinder S. Dahiya, Maurizio Valle, "Spice model for piezoelectric bender generator", IEEE, pp. 587-590, 2009.

[8] S. Priya, D. J. Inman, "Energy harvesting technologies", Springer, 2009.

[9] S. Roundy, „On the effectiveness of vibration-based Energy Harvesting", Journal of intelligent material systems and structures, Vol. 16, October 2005.

[10] P. M. Weaver, M. G. Cain, M. Stewart, ENG-02 Metrology for Energy Harvesting, WP 4: Piezoelectric and magnetic materials for energy harvesting from macro to nano-scale devices, M06 Progress review.

[11] Experimental Characterization of Thermoelectric Modules and Comparison with Theoretical Models for Power Generation, Emil Sandoz-Rosado and Robert J. Stevens. (2009)

[12] L Rauscher, S Fujimoto, H T Kaibe and S Sano, "Efficiency determination and general characterization of thermoelectric generators using an absolute measurement of the heat flow". IOPScience. (2005)

[13] D.M Rowe, "Handbook of thermoelectrics", CRC Press, 1995.

[14] Laurie Winkless, Miguel Munoz, Alexandre Cuenat, "Conversion efficiency of thermoelectric module", Open KM.

[15] S. Priya, D. J. Inman, "Energy harvesting technologies", Springer, 2009.

[16] Johannes de Boor and Volker Schmidt, "Complete characterization of thermoelectric materials by a combined van der Pauw approach", Adv. Mater. 2010, 22, 4303-4307.

[17] Shinichi Fujimoto, Hiromasa Kaibe, Seijirou Sano and Tsuyoshi Kajitani, "Development of Transient Measurement Method for investigating Thermoelectric Properties in High Temperature Region", Japanese Journal of Applied Physics, pp. 8805–8809, Vol. 45, No. 11, 2006.

[18] Jing-Feng Li, Wei-Shu Liu, Li-Dong Zhao and Min Zhou, "High-performance nanostructured thermoelectric materials", *NPG Asia Mater.* **2**(4) 152–158 (2010).

[19] Fraunhofer Institute for Physical Measurement Techniques IPM, http://www.ipm.fraunhofer.de

[20] Book Section, 2007, 978-0-387-28667-9; Scanning Probe Microscopy, Kalinin, Sergei, Gruverman, Alexei; 10.1007/978-0-387-28668-6_3; Probing Semiconductor Technology and Devices with Scanning Spreading Resistance Microscopy; http://dx.doi.org/10.1007/978-0-387-28668-6_3 , Springer New York, 2007-01-01, A Eyben, P. , Vandervorst, W. , Alvarez, D. , Xu, M. , Fouchier, M. , 31-87

[21] Precision and accuracy of thermal calibration of atomic force microscopy cantilevers G. A. Matei et al; Review of Sientific Instruments, Volume 77(8) 2006

[22] ISO/TC201/SC9 ISO 13089

[23] Karami, M. A. & Inman, D. J. Powering pacemakers from heartbeat vibrations using linear and nonlinear energy harvesters Applied Physics Letters, AIP, 2012, 100, 042901

[24] Stewart, M.; Weaver, P. M. & Cain, M. Applied Physics Letters, 2012, 100, 073901

[25] Briscoe, J.; Jalali, N.; Wolliams, P.; Stewart, M.; Weaver, P.; Cain, M. & Dunn, S. Measurement techniques for piezoelectric nanogenerators Energy Environ. Sci., 2013